



CSIRO

CSIRO LAND and WATER



---

# **The efficacy of vegetation in limiting spray drift and dust movement**

---

**Michael. R. Raupach and John F. Leys**

---

**Technical Report 47/99, October 1999**

---

# THE EFFICACY OF VEGETATION IN LIMITING SPRAY DRIFT AND DUST MOVEMENT

M.R. Raupach<sup>1</sup> and J.F. Leys<sup>2</sup>

<sup>1</sup>CSIRO Land and Water, GPO Box 1666, Canberra, ACT 2601, Australia  
<michael.raupach@cbr.clw.csiro.au>

<sup>2</sup>Department of Land and Water Conservation, PO Box 462, Gunnedah, NSW 2380, Australia  
<[jleys@dlwc.nsw.gov.au](mailto:jleys@dlwc.nsw.gov.au)>

**Summary:** This is a modelling investigation of the effects of riparian vegetation and other kinds of vegetative buffer areas on the movement of airborne particles such as drifting spray and dust. The aim is to provide guidelines specifying the properties of vegetation in buffer areas (including the extent of the buffer area and the height, leaf size, and density of the vegetation) which minimise the deposition of particles to sensitive environments downwind.

Vegetation can be used to protect sensitive receptor surfaces against particle deposition in two ways: *regional protection*, which occurs when particles are deposited to buffer vegetation and hence removed from the air flow *over* an extensive buffer area; and *local protection*, which occurs by particle deposition or filtering as air flows *through* a single porous vegetative barrier. Regional protection is most effective when the buffer vegetation is close to the particle source, whereas local protection is most effective when the porous vegetative barrier is close to the receptor. Most of this report is focused on regional protection.

The following preliminary guidelines are offered:

1. *Desirable characteristics of buffer vegetation for particle capture:* Buffer vegetation should be as aerodynamically rough as possible. Leaves should be as fine as possible.
2. *Placement of buffer vegetation:* From the viewpoint of regional protection, a limited area of buffer vegetation with a high potential for particle capture is most effective when it is close to the source, and least effective when it is close to the receptor.
3. *Anticipated quantitative reductions in particle deposition:* When placed close to a sprayed field, a shrub buffer area with an along-wind length of a few hundred metres can reduce deposition to a downwind receptor by 20% to 50%, relative to the deposition that would occur if the buffer area were pasture. These figures apply in neutral atmospheric stability conditions (occurring when wind speeds are high); much greater reductions are obtained in strongly stable conditions (occurring mainly on calm nights). Since the risk of deposition is higher in strongly stable than in neutral conditions, the benefits of buffer vegetation are greatest when they are most needed.
4. *Role of local protection:* Local protection against particle deposition by a porous barrier extends downwind from a windbreak or tree belt for a distance of 5 to 10 tree heights. Local protection is generally most effective when the protecting barrier is close to the receptor.

In a concluding section, the report offers an assessment of the reliability of different aspects of the present modelling work; an assessment of possible future research directions; and a brief assessment of the implications of these results for resource equity.

## 1 Introduction

There is community and government concern over the detection of pesticides, particularly endosulfan, in rivers and cattle in the cotton-growing regions of northern New South Wales. For contamination to occur, the pesticide needs to be transported from the site of application to the receptor site. The pathways by which such transport can occur were investigated in the recently completed research and development program “Minimising the Impact of Pesticides in the Riverine Environment” (Schofield *et al.* 1999). Within this program, a modelling study (Raupach *et al.* 1999a,b) identified and quantified four major pathways: (1) spray drift, (2) vapour transport, (3) dust transport (all airborne pathways) and (4) runoff (a waterborne pathway). The major findings included: (1) spray drift, vapour transport and runoff are all significant pathways for transport over distances of kilometres; (2) dust transport is less significant for transport over these distances, but can be significant for shorter-range (on-farm) transport; (3) spray drift and vapour transport both contribute low-level but nearly continuous inputs of endosulfan to the riverine environment during spray season in a large cotton-growing area, whereas runoff provides occasional but higher inputs. These studies also have implications for transport to pastures and thence to cattle, for which airborne pathways are likely to be the dominant transport routes. In summary, the aerial transport and deposition of spray droplets and dust is a significant pathway for the movement of agricultural chemicals, with potential adverse effects on sensitive areas such as riverine environments or grazing land used to produce cattle for both domestic and international human consumption.

It is widely believed that the deposition of particles to sensitive areas can be greatly reduced by vegetation, including windbreaks and buffer strips which can be either purpose-planted or formed by retaining native vegetation. (In this report, the term “particles” will include both spray droplets and dust). However, little quantitative guidance is available to assess the effectiveness of vegetation in reducing downwind particle deposition. One reason for this lack of information is that windbreaks and buffer strips almost always provide a scattered or patchy vegetative cover on a landscape, a factor which has major implications for efficacy of the vegetation in capturing particles by deposition to the surface. There is almost no extant literature on the deposition of particles to patchy vegetation. In contrast, there is a significant base of knowledge about particle deposition to extensive, *uniform* vegetation canopies (eg. Sehmel 1980, Slinn 1982, Davidson and Wu 1990, Raupach *et al.* 1999b). There is also some knowledge of the aerodynamic drag properties of scattered or patchy vegetation

(eg. Arya 1975, Raupach 1992, 1994) and the air flow around windbreaks (eg. Judd *et al.* 1996). This provides guidance about the likely behaviour of particle deposition to patchy surfaces and to windbreaks, because there are strong (though far from complete) similarities between the processes of particle deposition and momentum absorption on vegetation.

This report is a first attempt to provide a quantitative model for the removal of particles from the air by patchy vegetation, and the subsequent effect on particle deposition to downwind surfaces. The theory and modelling framework is very simple and approximate (this work is the modelling equivalent of carpentry, not joinery). Also, many of the predictions have not been tested by experimental data because such data do not yet exist. For both reasons, the conclusions of the report need to be interpreted as hypotheses rather than firm, quantitative predictions. However, we assess the likely reliability of our conclusions whenever possible. Because of the new science involved, the findings of this project will be submitted to internationally refereed journals in due course. Meanwhile, this report provides preliminary guidelines on the optimum ways that vegetation can be maintained or planted in the landscape to minimise the off-site movement of particles, including spray drift and dust.

The first objective of this report is to formulate such preliminary guidelines. The second is to assist the vegetation reform process of the NSW Department of Land and Water Conservation (DLWC) by providing these guidelines in a form which can be used by the vegetation management officers of DLWC and the vegetation management committees who are currently trying to implement the Native Vegetation Conservation Act 1998. The final objective is to contribute to one of the corporate goals of the DLWC: “to improve the health and productivity of the ecosystems of NSW”. The findings of this report indicate ways to enhance the health of river systems and adjacent terrestrial ecosystems, by minimising the off-site movement of pesticides from agricultural operations.

The plan of the report is as follows. After this introduction, Section 2 summarises some concepts and physical theories used in the work. Section 3, the main part of the report, then covers (in 3.1) a model for the influence of broad patches of vegetation on downwind particle deposition; (3.2) tests of the model against the limited available data; (3.3) analysis of model assumptions; (3.4) scenarios for model application; and (3.5) model results. Finally, Section 4 gives conclusions and recommendations. Mathematical and other details are relegated to three Appendices.

## 2 Basic Principles of Particle Deposition to Vegetation

### 2.1 Regional and Local Influences of Vegetation on Particle Deposition

We are concerned with the deposition of particles to downwind vegetated surfaces from upwind sources such as sprayed cotton fields or dust sources. Horizontal position will be defined by coordinates  $x$  and  $y$ , with axes aligned along the wind ( $x$ ) and across the wind ( $y$ ). Height will be denoted  $z$ , with  $z = 0$  at the ground. Most of the report is restricted to the laterally homogeneous situation in which both the source for particle emissions and also the downwind surface are uniform in the lateral ( $y$ ) dimension, consisting of long cross-wind strips. In this situation, the source distribution and the deposition pattern are independent of  $y$ , and the deposition pattern depends spatially on  $x$  only.

The processes by which vegetation provides protection against particle deposition further downwind can be idealised in two different ways, acting respectively at regional and local scales. These are shown schematically in Figures 1 and 2.

**Regional protection** occurs when particles are extracted from the air flowing over an extensive "buffer" area with a high potential for absorbing particles, such as a wide vegetative buffer strip. The mechanism for this type of protection is as follows:

1. A relatively deep layer of particle-laden air, tens to hundreds of metres deep, is assumed to be produced by a particle source some distance upwind. The further upwind the source, the deeper is this layer. This incident flow is represented by point A in Figure 1.
2. The particle-laden air encounters a highly absorbing buffer surface, typically consisting of relatively tall vegetation with fine leaves (optimal vegetation characteristics for particle absorption are discussed in Section 2.3). Particles are mixed downwards and deposited to this buffer surface, reducing particle concentrations in a "scrubbed" air layer which deepens with increasing distance ( $x$ ) across the buffer surface; see point B in Figure 1.
3. Beyond the buffer surface, deposition to the downwind receptor surface is reduced. This occurs both because of the low particle concentrations in the scrubbed air layer itself (a relatively short-range effect), and also because particle concentrations in the entire particle-bearing layer are reduced by mixing and dilution of the remaining particle-laden air with the relatively clean air in the scrubbed layer (a long-range effect).

**Local protection** occurs when particles are filtered out of the air flowing *through* a porous vegetative barrier such as a windbreak or narrow buffer strip. The barrier, of height  $H$ , is

assumed to be long in the cross-wind ( $y$ ) direction and narrow in the along-wind ( $x$ ) direction, and to be located at  $x = 0$ . The mechanism is as follows (Figure 2):

1. As in the regional case, we assume that the porous barrier is immersed in a particle-laden air flow which is much deeper than the height  $H$  of the barrier itself, so that the incident particle concentration is approximately uniform with height; see point A in Figure 2.
2. Some of the oncoming air is filtered through the barrier while some passes over it. Particle concentrations are not changed in the air flowing over the barrier, but are strongly reduced in the through-flowing "bleed flow" by absorption onto leaves and stems in the barrier; see point B in Figure 2. There is a strong reduction in particle deposition to the surface in the immediate lee of the barrier, caused both by the reduced particle concentration and the reduced wind speed in this region, which corresponds with the "quiet zone" in the lee of the barrier. This region extends to a distance  $x$  of around  $5H$  to  $10H$  from the barrier. There is also a large deposition of particles to the barrier itself, more than compensating for the reduced deposition in the quiet zone.
3. Particles in the flow above the barrier are mixed downwards into the quiet zone with increasing distance ( $x$ ) from the barrier. Hence, near-surface particle concentrations and surface deposition both increase, eventually recovering approximately to their values upwind of the barrier. The local protection provided by a single barrier therefore effectively reduces deposition in the immediate lee of the barrier, but does not have much impact on concentrations further downwind.

In summary, regional protection occurs by downward deposition from the air flowing *over* an extensive buffer area; while local protection occurs by deposition or filtering as air flows *through* a single porous barrier. The distinction between the two mechanisms is not absolute, because repeated porous barriers (each providing local protection in its immediate lee) can constitute a buffer area which provides regional protection by scrubbing and diluting the particle-laden flow above. However, the distinction is useful because different modelling approaches are appropriate for the two cases.

This focus of this report is on *regional* protection. A full quantitative assessment of local protection lies outside the present scope. Before describing the modelling framework, the rest of this section introduces some basic concepts applicable at both regional and local scales.

## 2.2 Definitions of Deposition, Dose Concentration and Deposition Velocity

We will consider a finite release of particulate material such that the source of airborne particles is confined to a small interval of time, as in a single spray event on a cotton field. Such a source is known as an “instantaneous puff” release. The resulting total particle deposition on any downwind receptor surface is expressed in units of mass per unit ground area ( $\text{kg m}^{-2}$ ) and is denoted  $D$ . It is equal to the time integral of the downward flux of particles to the surface,  $-\mathbf{f}$  ( $\text{kg m}^{-2} \text{s}^{-1}$ , with  $\mathbf{f}$  being the upward flux). The dose (or dose concentration)  $C$  from a puff release can likewise be defined as the accumulated concentration at any point throughout the passage of the puff, or the time integral of the actual, time-dependent concentration  $c$ . Hence:

$$D(x, y) = - \int_{-\infty}^{+\infty} \mathbf{f}(x, y, t) dt ; \quad C(x, y, z) = \int_{-\infty}^{+\infty} c(x, y, z, t) dt \quad (1)$$

where  $x$  and  $y$  are horizontal coordinates (as above) and  $t$  is time. The units of  $C$  are concentration  $\times$  time, or  $\text{kg m}^{-3} \text{s}$ . Throughout this report, dose defined in this way will be the basic measure of concentration.

The deposition flux to an underlying surface ( $-\mathbf{f}$ ) can be related to the concentration  $c_r$  at a reference point just above the receptor surface by a *deposition velocity*  $W_d$ , such that

$$-\mathbf{f} = W_d c_r \quad (2)$$

The deposition velocity has units  $\text{m s}^{-1}$  and is a parameter describing the efficiency of the underlying surface in capturing particles from the flow above it. Formally,  $W_d$  is an aerodynamic conductance for particle transfer from the flow to the surface, under the assumption that  $c$  is zero at the surface. If  $W_d$  is constant in time (which happens if the wind speed and atmospheric stability do not change through the passage of the puff), then Equation (2) can be integrated in time to give

$$D = W_d C_r \quad (3)$$

so that total deposition is related to dose in the same way as deposition flux to concentration.

## 2.3 Model for Deposition Velocity

The deposition of particles to a vegetated surface occurs by three processes acting in parallel: direct gravitational settling to the surface, inertial impaction of particles on individual elements (leaves and stems), and Brownian diffusion of particles through the boundary layers

of individual elements. All of these processes are strong functions of particle diameter: gravitational settling dominates for large particles ( $> 100 \mu\text{m}$ ), impaction in a middle size range centred around  $10 \mu\text{m}$ , and Brownian diffusion for very small particles ( $\ll 1 \mu\text{m}$ ). The deposition velocity  $W_d$  is therefore a complicated function of the particle diameter, with a minimum at around  $1 \mu\text{m}$  where none of the three processes is effective. Impaction and Brownian diffusion are also strong functions of the length scale of the canopy elements (such as a leaf width or stem diameter) and the local wind speed.

The model used for  $W_d$  in this report is the same as in Raupach *et al.* (1999b), and is described in Appendix A. It is a "single-layer" model in which the deposition velocity is treated as a bulk (single-layer) conductance made up of three parallel components:

$$W_d = W_t + G_{imp} + G_{brow} \quad (4)$$

where  $W_t$  (the terminal velocity) accounts for gravitational settling,  $G_{imp}$  for impaction, and  $G_{brow}$  for Brownian diffusion. Of these three,  $W_t$  is a well-known function of particle diameter, particle-to-air density ratio and air viscosity (Malcolm and Raupach, 1991). Both  $G_{imp}$  and  $G_{brow}$  are calculated by utilising the substantial (but not complete) similarities between the transfer processes involved in particle deposition and in momentum absorption or drag. The eventual form of the model is Equation (A5) in Appendix A.

Some tests and results of this model are shown in Figures 3 to 5. First, Figure 3 shows a test of the model against the classical wind tunnel data set of Chamberlain (1967), for deposition of particles of various sizes to sticky (artificial) short grass of height  $0.06 \text{ m}$ . The model reproduces the main features of the variation of  $W_d$  with particle diameter  $d$ , especially the minimum in  $W_d(d)$  around  $d = 1 \mu\text{m}$  and the convergence of  $W_d$  to the settling velocity  $W_t$  for large particles. The model also satisfactorily reproduces the trend of the data with wind speed. Given the simplicity of the model, this level of agreement is quite satisfactory.

Figure 4 shows typical contributions of the three terms  $W_t$ ,  $G_{imp}$  and  $G_{brow}$  to  $W_d$ , over the particle size range  $0.01$  to  $1000 \mu\text{m}$ . The significant range for spray drift is broadly  $10$  to  $1000 \mu\text{m}$ . For particles around  $10 \mu\text{m}$  impaction is the dominant process contributing to  $W_d$ , and around  $1000 \mu\text{m}$ ,  $W_d$  is dominated by particle settling.

Figure 5 shows the dependence of  $W_d$  on particle size, leaf dimension, vegetation height, Leaf Area Index (LAI) and wind speed, for typical field situations specified in the figure caption. (The interpretation of LAI for sparse canopies is discussed in Appendix C, by

relating LAI to other measures such as plant density in stems per unit area.) In the particle size range from 3 to 100  $\mu\text{m}$ ,  $W_d$  increases as leaf dimension ( $d_c$ ) decreases (Figure 5a); increases as canopy height ( $h_c$ ) increases (Figure 5b); and increases as reference wind speed ( $u_r$ ) increases (Figures 3 and 5c). Also,  $W_d$  exhibits a peaked behaviour as a function of LAI, peaking near LAI = 1 (Figure 5c). This is consistent with a similar peak for momentum transfer (Raupach 1992, 1994).

### 3 Regional Influence of Vegetation on Particle Deposition

#### 3.1 Model for Particle Deposition to Nonuniform Vegetation

To assess regional protection against particle deposition, it is necessary to describe the dispersion and deposition of a cloud of particles over a patchy or heterogenous surface. We consider mainly the laterally homogeneous case in which the deposition velocity  $W_d$  varies with streamwise distance ( $x$ ) but not lateral position ( $y$ ). Likewise the deposition  $D(x)$  is a function of  $x$  only. We require a means of predicting  $D(x)$ , for any specified distribution of particle sources and downwind surfaces, the latter characterised by specifying  $W_d(x)$ .

The model used here for this purpose is a simple, approximate description based on mass conservation and a Gaussian-plume assumption. The model, described fully in Appendix B, has been adapted from a comparable model for deposition to a uniform downwind surface (Raupach *et al.* 1999b). In brief, the model determines the deposition  $D(x)$  from a plane particle source of strength  $Q$   $\text{kg m}^{-2}$ , extending from  $-x_p$  to 0 in the  $x$  direction. This is expressed as a "deposition fraction"  $D(x)/Q$ , the deposition normalised by the plane source strength, where both  $D(x)$  and  $Q$  are in  $\text{kg m}^{-2}$ . In the case of a spray application,  $Q$  is the intended dose of spray on the target field and  $D(x)/Q$  is the "drift deposition fraction"  $f_{drift}$  defined in Raupach *et al.* (1999a,b). The model expresses  $D(x)/Q$  as the sum of the depositions  $D_1(x|x_s)$  from a series of unit lateral line sources at locations  $x_s$ :

$$f_{drift} = \frac{D(x)}{Q} = \int_{-x_p}^0 D_1(x|x_s) dx_s \quad (5)$$

A unit lateral line source is a particle release of 1 kg per y-metre along a line across the wind at location  $x_s$ . Its deposition field  $D_1(x|x_s)$  is given by

$$D_1(x|x_s) = W_d(x) C_1(x|x_s); \quad C_1(x|x_s) \sim \frac{s(x|x_s)}{u_r \mathbf{S}_Z(x-x_s)} \quad (6)$$

where  $C_1(x|x_s)$  is a low-level dose concentration (at location  $x$  and at the reference height  $z_r$ ) from the unit lateral line source at  $x_s$ ;  $s(x|x_s)$  is the mass fraction in a puff at  $x$  after release at  $x_s$ ;  $u_r$  is a reference wind speed; and  $\sigma_Z(x-x_s)$  is the depth at  $x$  of the cloud of particles released at  $x_s$  (a function of  $x-x_s$  only because the cloud is assumed to grow at a specified steady rate). The key quantity is the mass fraction  $s(x|x_s)$ , a dimensionless quantity between 0 and 1 equal to the mass of particles passing the point  $x$  as fraction of the original mass released at  $x_s$ . It is determined by a linear ordinary differential equation of the form

$$\frac{ds(x|x_s)}{dx} \sim \frac{W_d(x)s(x|x_s)}{u_r \sigma_Z(x-x_s)} \quad (7)$$

Equations (6) and (7) give only the essential order-of-magnitude behaviour of  $s(x|x_s)$ . The full equations are given in Appendix B, Equations (B10) and (B8). This model is based on the "source-depletion" approach (Hanna *et al.* 1982). Its key assumptions are stated and analysed below, after describing the basic behaviour of the model and presenting an experimental test for the case of deposition to a uniform surface, where  $W_d(x)$  is constant.

### 3.2 Model Behaviour and Field Tests for Uniform Vegetation

The basic behaviour of the model is shown in [Figure 6](#) by plotting the depleting mass fraction  $s(x)$ , the deposition  $D_1(x|x_s)$  for a unit lateral line source at  $x_s = 0$ , and the deposition fraction  $f_{drift} = D(x)/Q$  for a plane source for several particle size distributions, all for the case of deposition to a uniform surface with constant  $W_d$ . The effect of increasing particle size in limiting downwind deposition is evident.

The model has been compared with field data from Bird *et al.* (1996) on the deposition of spray drift to a uniform downwind surface; see Raupach *et al.* (1999b) for details. [Figure 7](#) compares the field data of Bird *et al.* (who used a spray with a median droplet diameter of close to 250  $\mu\text{m}$ ) with the model predictions for the deposition fraction  $D(x)/Q$  at three wind speeds, using model parameters selected to match the experimental conditions. The predictions capture both the magnitude and the streamwise trend of  $D(x)/Q$  very well, slightly overestimating the magnitude of  $D(x)/Q$  at higher wind speeds (at most by about 20%). Given the major simplifications of the model, this is a very satisfactory result.

### 3.3 Analysis of Model Assumptions

As stated in more detail in Appendix B, the above model for particle deposition to patchy vegetation involves two key assumptions:

1. At each  $x$ , the dose concentration field  $C(x,y,z)$  in the dispersing and depositing puff is equal to that in a non-depositing but otherwise similar puff, multiplied by the mass fraction  $s(x/x_s)$ ;
2. The shape of  $C(x,y,z)$  is Gaussian in space, with reflection at the ground.

Of these, Assumption 1 is reasonable on mass conservation grounds; in fact, Equation (B5) in Appendix B shows that Assumption 1 is exact in an integral sense when the wind speed is independent of height. However, Assumption 2 is a major simplification of the real physics. The real content of Assumption 2 is not the use of a Gaussian form for  $C(x,y,z)$ ; rather it is the assumption that  $C(x,y,z)$  is self-similar in  $z$  (except within a short distance of an elevated source, of order  $h_s\sigma_w/u_r$ , in which the plume contacts the ground). This means that the dose concentration fields  $C(x,y,z)$  at different values of  $x$  can all be collapsed to a single shape, or function of  $y$  and  $z$ , by stretching or rescaling this common function with scaling factors dependent on  $x$ . The self-similar assumption leads to the order-of-magnitude results for  $C_1(x|x_s)$  and  $ds/dx$  in Equations 6 and 7. The more specific assumption of a Gaussian  $C(x,y,z)$  is merely a special form of self-similarity which enables the dimensionless coefficients in these relationships to be determined easily, as in Appendix B, Equations (B10) and (B8).

For the case of uniform downwind vegetation, where  $W_d$  is independent of  $x$ , the behaviour of  $C(x,y,z)$  is probably quite close to self-similar even for a strongly settling plume, a viewpoint supported by the excellent agreement (Figure 7) between theory and experimental results for uniform downwind vegetation. However, for nonuniform downwind vegetation, when  $W_d$  changes with  $x$ , the shape of the vertical profile of  $C$  may change substantially with increasing  $x$ , as indicated qualitatively in Figure 1. This means that  $C(x,y,z)$  is not self-similar. The effect of imposing a self-similar behaviour (as done by our simple theory) is to smooth the vertical structure of the real concentration profiles, for instance at point B in Figure 1. This will cause the modelled near-surface concentration ( $C(x,y,z_r) = C_r$ ) and deposition ( $D = W_d C_r$ ) to respond more slowly to changes in  $W_d$  than would occur in reality. Thus, for example, the model is incapable of reproducing an increase in  $C_r$  and  $D$  just downwind of a high- $W_d$  buffer surface (as sketched between points B and C in Figure 1) because it cannot incorporate the downward mixing of high concentrations from above which lead to this behaviour.

Nevertheless, there are two situations in which the self-similar assumption, and hence Equations (6) and (7), are likely to be justifiable even over nonuniform vegetation. The first is

when mixing is so efficient that local bumps in  $C(x,y,z)$  (as at point B in Figure 1) are rapidly smoothed out over entire depth of the particle-bearing layer. This happens when  $\sigma_w$ , the standard deviation of the vertical turbulent velocity in the air, is much larger than the non-settling part of the deposition velocity ( $W_d - W_t = G_{imp} + G_{brow}$ ). Such a situation is often approximated in practice, especially over rough surfaces where  $\sigma_w$  is increased relative to flow over smoother surfaces. The second favourable situation for self-similarity occurs when the changes in the profile shapes are relatively small, which happens when the surface is absorbing little material from the plume compared with the amount present, so that  $\Delta x ds/dx$  is small over a significant distance  $\Delta x$ .

In summary, despite major simplifications, there are reasons for suggesting that the present simple model may give reasonable guidance about the effects of regional protection on deposition, or in other words, the effect of variation in  $W_d(x)$  on  $D(x)$ . More sophisticated models are both possible and desirable to construct, to test the extent to which the simplifications in the present approach can be supported.

### 3.4 Model Scenarios

The model described in the foregoing subsections has been used to predict the deposition of a cloud of particles over a range of alternative vegetated buffer surfaces occupying a "buffer area" between a particle "source area" and a downwind "receptor area". The scenarios used in the model tests are illustrated in *Figure 8*, and are defined as follows:

- We consider only the laterally homogeneous case in which all quantities vary with streamwise distance ( $x$ ) but not lateral position ( $y$ ). Thus the source, buffer and receptor areas are all considered to be long strips oriented at right angles to the wind direction.
- The plane source of particles has an along-wind length  $x_p$  of 1000, 100 or 10 m. These lengths correspond approximately to a large sprayed cotton field, a small sprayed horticultural field or a single swathe of spray. The downwind edge of the source is always at  $x = 0$ , so that  $x_p = -1000$  m,  $-100$  m or  $-10$  m for the three source dimensions.
- The particles are of uniform diameter  $d$ , either "spray" with  $d = 80 \mu\text{m}$  and a release height  $h_s$  of 2 m (representing a ULV spray applied to a cotton crop); or "dust" with  $d = 30 \mu\text{m}$  and  $h_s = 0$  (representing a typical local dust source from an area bare of

vegetation). The terminal fall velocities ( $W_t$ ) of water droplets with diameters of 80 and 30  $\mu\text{m}$  are respectively 0.18 and 0.027  $\text{m s}^{-1}$ .

- Table 1 gives the surface properties (height  $h_c$ , leaf area index LAI and leaf breadth  $d_c$ ) assumed for the plane source area, which influence particle deposition to the source area itself. Different properties are assumed for "spray" and "dust" sources.
- The receptor (the surface to be protected against particle deposition by buffer vegetation) is always an idealised "pasture" surface with properties ( $h_c$ , LAI and  $d_c$ ) given in Table 1. The receptor area is always between distances  $x = 800$  m and 1000 m downwind of the lee edge of the source area. We use the deposition at  $x_p = 1000$  m as a measure of the deposition to the receptor.

Surface	Context	Canopy height $h_c$ (m)	LAI	Leaf size $d_c$ (m)	Deposition velocity $W_d$ ( $\text{m s}^{-1}$ )	
					"Spray"	"Dust"
Cotton	"Spray": source area surface	0.5	3	0.01	0.189	
Bare surface	"Dust": source area surface	-	-	-		0.0270
Shrub	Buffer surface	2	1	0.003	0.245	0.0540
Pasture	Buffer and receptor surface	0.1	3	0.01	0.181	0.0273

Table 1: Surfaces used in tests of effects of alternative vegetated buffer surfaces between a particle source and a downwind receptor. Deposition velocities to the surfaces are given for the standard meteorological conditions defined in the text (wind speed  $u_r = 5$   $\text{m s}^{-1}$  at a reference height  $z_r = 10$  m, and atmospheric neutral stability).

- The surface cover in the buffer area (between  $x = 0$  and 800 m) takes several alternative forms, made up of just two alternative idealised vegetation types "pasture" (P), similar to the receptor surface, or "shrub" (S), a buffer surface designed to have a high deposition velocity and hence a high potential for particle capture. The assumed properties of both surface types are given in Table 1. These surface types are arrayed in the following alternative "buffer configurations" (see Figure 8):

- S: shrub throughout the strip between  $x = 0$  and 800 m
- P: pasture throughout the strip between  $x = 0$  and 800 m
- SP: shrub (0 to 400 m), pasture (400 to 800 m)
- PS: pasture (0 to 400 m), shrub (400 to 800 m)
- SPS: shrub (0 to 200 m), pasture (200 to 600 m), shrub (600 to 800 m)
- PSP: pasture (0 to 200 m), shrub (200 to 600 m), pasture (600 to 800 m)

Configurations P and S are single-surface buffer strips, whereas the others are dual-surface buffer strips consisting of 400 m of shrub and 400 m of pasture, arrayed in four alternative ways with the shrub component respectively as close as possible to the source (SP), as close as possible to the pasture receptor (PS), divided so that some shrub is close to the source and some to the receptor (SPS), and concentrated in the middle of the buffer area, with pasture on either side (PSP).

- Assumed meteorological conditions are a wind speed  $u_r = 5 \text{ m s}^{-1}$  at a reference height  $z_r = 10 \text{ m}$ , and neutral stability (except for tests of the effect of stability described below).

### 3.5 Model Results

The model for particle deposition to nonuniform vegetation has been applied to calculate deposition to the buffer area and the receptor area for all the configurations described above.

Figure 9 illustrates the most detailed level of information produced by the model. It shows typical results for the deposition fraction  $D(x)/Q$  as a function of  $x$ , for all six buffer configurations, in the case of a spray source (particle diameter  $d = 80 \text{ }\mu\text{m}$ ), with along-wind length  $x_p = 10 \text{ m}$  (a single-swathe), under the typical meteorological conditions specified above (in particular, with neutral atmospheric stability). For clarity the results are shown in two panels: Figure 9a includes configurations P, S, SP and PS, while Figure 9b shows configurations SPS and PSP (together with P and S, repeated for reference). Note that the vertical axis is logarithmic and covers a range of three decades or a factor of  $10^3 = 1000$ .

Several features emerge from Figure 9:

- (a) The deposition over the pasture receptor ( $x = 800$  to  $1000 \text{ m}$ ) is largest when the buffer area is entirely pasture (configuration P), and smallest when it is entirely shrub (configuration S). The deposition to the pasture receptor is about a factor of 2 lower when the buffer area is entirely shrub (S) than when it is entirely pasture (P), with all other properties of the source and receptor surface held constant.

- (b) The reduced deposition on the receptor at 1000 m in configuration S, relative to configuration P, is the result of a higher deposition to the shrub than to the pasture in the buffer area just downwind of the source, in the range  $x = 0$  to 200 m. (This is a little difficult to see in Figure 9 because of the logarithmic scale, which is necessary to show the critical differences in the small depositions to the receptor at  $x = 1000$  m among the various configurations). The higher deposition to shrub near the source occurs because the shrub removes particles much more effectively from the atmosphere, as reflected by its higher deposition velocity  $W_d$  (see Table 1). Hence, the low-level particle concentration ( $C_r$ ) falls more rapidly over the shrub than the pasture. Since the deposition  $D = W_d C_r$ , the result is lower deposition for configuration S than configuration P to surfaces further downwind than the initial high-deposition region, including the receptor at  $x = 1000$  m.
- (c) Configurations SP, PS, SPS and PSP (all of which involve 400 m of shrub) produce varying reductions in deposition at the pasture receptor ( $x = 1000$  m), in the following order: SP, SPS, PSP, PS (from lowest to highest deposition to the receptor, or largest to smallest reduction in deposition relative to configuration P). The role of the shrub surface in producing these reductions is evident from the enhanced deposition to the shrub relative to the pasture, visible from the steps in  $D(x)/Q$  at the boundaries of the shrub surfaces.
- (d) The general conclusion from point (c) is that *from the viewpoint of regional protection, a limited area of buffer vegetation with a high potential for particle capture is most effective when it is placed close to the source, and least effective when it is close to the receptor.* The reason is that particle concentrations decrease with increasing distance downwind from the source, both because of deposition to the surface and because the depth of the particle-laden air layer increases. Since the deposition  $D = W_d C_r$ , a higher deposition to the shrub and therefore greater particle removal is achieved by placing the shrub close to the source, where  $C_r$  is high, than close to the receptor where  $C_r$  is lower.

Figure 10 provides a simpler, bar-chart comparison of the depositions to the pasture receptor surface at  $x = 1000$  m, for all six buffer configurations S, P, SP, PS, SPS, PSP. Results are shown for the three different source lengths ( $x_p = 10, 100$  or  $1000$  m, as separate bars for each configuration) and for spray and dust particles (in Figures 10a and 10b, respectively). The points emerging from Figure 10 (continuing the previous list) are:

- (e) In all cases, conclusions (c) and (d) are supported: that is, the effectiveness of the buffer configurations in reducing particle deposition to the receptor runs in the order S, SP, SPS,

PSP, PS, P (best to worst protection), and a given area of buffer vegetation with a high potential for particle capture is best placed near the source.

- (f) For all buffer configurations, the magnitude of the reduction in particle deposition (relative to the deposition for a pasture buffer, case P) is greatest for small area sources ( $x_p = 10$  m) and smallest for large area sources ( $x_p = 1000$  m). The reason is similar to that underlying point (c): for large sources (say  $x_p = 1000$  m), particles contributed by upwind parts of the source are dispersed through quite a deep particle-laden air layer by the time they encounter the buffer vegetation, so they are quite dilute and are not efficiently captured (recalling that the deposition  $D = W_d C_r$  is proportional to the concentration).
- (g) Figure 10 suggests that for a large source area such as a cotton field with  $x_p = 1000$  m, the overall reductions in deposition obtained by the use of buffer vegetation are modest: for instance, configuration S (800 m of shrub in the buffer area) produces only 30% less deposition than configuration P (a buffer area entirely planted to pasture). However, this impression is not entirely accurate because both Figures 9 and 10 are confined to neutral atmospheric stability.

Figure 11 shows the effect of atmospheric stability on the deposition on the receptor at  $x = 1000$  m, for the shrub buffer (configuration S). Atmospherically stable conditions arise when warm air overlies cool air, so that buoyancy forces suppress vertical mixing; this happens mainly on calm nights. Unstable conditions arise when cool air overlies warm air, so that the air column undergoes rapid vertical mixing driven by buoyancy forces; this occurs on hot days when the ground surface is much hotter than the air above.

The relative deposition plotted in Figure 11 is the deposition for configuration S normalised by the deposition for configuration P under similar stability conditions, so the figure shows the influence of stability on the deposition reduction at the receptor achieved by vegetating the entire buffer area with shrub rather than pasture. Results are shown for three different atmospheric stabilities: strongly unstable (stability class A), neutral (class D) and strongly stable (class F). The important conclusion from Figure 11 is:

- (h) The effect of a buffer of highly absorbing vegetation in reducing deposition to a downwind receptor increases dramatically in stable atmospheric conditions (mainly on calm nights). Particle dispersion in these conditions (from sources such as spraying or vehicular dust) leads to particularly high concentrations and deposition downwind, because the suppression of vertical mixing in stable conditions confines the particle-laden

air layer close to the ground. For the same reason, the efficacy of buffer vegetation in providing regional protection is also increased. Hence, the efficacy of the buffer vegetation is greatest in the atmospheric stability conditions when it is most needed.

Finally we consider the effect of the density of the buffer vegetation, as quantified by the Leaf Area Index (LAI). Appendix C provides a brief description of the relationship of LAI to other measures of canopy density such as cover fraction, and some rough rules for deducing the LAI from simple visual measures such as the distance through the canopy over which 2/3 of a white card is obscured by intervening leaves and stems.

*Figure 12* shows the effect of the LAI of shrub vegetation in the buffer area, for configuration S. As before, the depositions are normalised by the deposition for a pasture buffer surface (configuration P). It is found that:

- (i) The reduction in deposition to the receptor (pasture at  $x = 1000$  m) imparted by a shrub buffer area (configuration S) is greatest when the LAI is near 1. Both smaller and larger LAI values lead to increased deposition to the receptor. This is consistent with the earlier finding that the deposition velocity  $W_d$  peaks at a LAI near 1, all other conditions being held constant (Section 2.3, Figure 5c).
- (j) The values in Figure 12 all pertain to neutral (class D) conditions of atmospheric stability. Much more protection would be obtained in strongly stable conditions, as in Figure 11.
- (k) When the LAI of the primary buffer vegetation (here, shrub) is too small, significant protection is not obtained. Although any LAI implies some protection, values of around 0.03 or larger are needed for a regional protection effect of 10% or more in neutral conditions. Rough estimates in Appendix C show that such an LAI corresponds with 50 to 100 trees per hectare with height and diameter around 2 m and medium foliage density.

#### **4 Conclusions, Guidelines and Recommendations for Further Work**

***Preliminary guidelines:*** The main results of the study are stated above in points (a) to (k).

These can be reduced to the following preliminary guidelines for the use of buffer vegetation in providing regional protection against particle deposition to downwind receptors:

1. *Desirable characteristics of buffer vegetation for particle capture:* Vegetation should be as aerodynamically rough as possible. This means that the height should be as tall as possible, and the Leaf Area Index (LAI) should be within or near an optimal range of order 0.3 to 1 (corresponding to a cover fraction of order 15% to 50%, according to very

rough approximations in the last paragraph of Appendix C). LAI values outside this range produce lower particle capture, as measured by the deposition velocity  $W_d$ . The leaves should be as fine as possible, for the most efficient possible particle capture.

2. *Placement of buffer vegetation:* From the viewpoint of regional protection, a limited area of buffer vegetation with a high potential for particle capture is most effective when it is placed close to the source, and least effective when it is close to the receptor.
3. *Anticipated quantitative reductions in particle deposition:* The present preliminary calculations suggest that, relative to a buffer area of pasture, regional protection by a shrub buffer area can reduce deposition to a downwind receptor by 20% to 50% in neutral atmospheric stability conditions, and by much more in strongly stable conditions when risk of deposition is higher.
4. *Role of local protection:* Local protection has not been modelled in this work, but it has been discussed briefly in Section 2.1. A simple guideline from knowledge of windbreak flows (Judd *et al.* 1996) is that local protection against particle deposition extends downwind from a windbreak or tree belt for a distance of 5 to 10 tree heights. This implies that *local protection is most effective when the buffer vegetation close to the receptor*, which is the opposite to the situation for regional protection.

***Likely reliability of conclusions:*** As indicated in this report, especially in Section 3.3, the present modelling project is based on some major simplifications of a complicated physical problem. The following assessments of reliability can be made:

- Broadly, we have confidence in the modelling of the deposition velocity of particles to vegetation, and hence the dependence of the potential of vegetation for particle capture on variables such as height, leaf dimension, LAI and wind speed. Although the model (Section 2.3 and Appendix A) is simple, it is robust and is verified by available data.
- Our model for particle dispersion and deposition is also regarded as adequate, *for deposition to uniform vegetation*. For this case it is supported by field data.
- However, we have "pushed the envelope" in applying this model to *nonuniform* vegetation. The biggest uncertainty is introduced by our assumption that concentration fields of depositing particle clouds are self-similar. This causes the modelled deposition to respond more slowly to changes in the deposition velocity  $W_d$  than would occur in reality, and prevents the model from reproducing an increase in deposition just downwind of a

high- $W_d$  buffer surface, as sketched between points B and C in Figure 1. This is one respect in which regional shelter may provide a local benefit which we cannot yet assess.

- We have also suggested a very rough framework (Appendix C) for relating LAI to geometrical properties of canopies. This should be used for rough field guidance only.

***Opportunities and need for further work:*** We believe that this work has opened an exciting new avenue of substantial practical importance. There are three main lines of further work that can usefully be pursued:

- *Further development of the theory for regional protection:* Many of the assumptions in this work (especially the assumption of self-similarity) can be supported or made unnecessary by more extensive treatments, especially by numerical methods for determining the advection, diffusion, settling and deposition of a cloud of particles.
- *Development of a theory for local protection:* There is a need to quantify Figure 2, beyond the simple statement in Guideline 4 above.
- *Experimental support:* Most importantly, there is a need for experimental data on both local and regional protection, to support or modify analyses such as this one.

***Implications for Resource Equity Issues:*** Finally, we have noted the existence of two different forms of vegetative protection against particle deposition: regional protection, most effective close to the source, and local protection, most effective close to the receptor. This raises issues of resource equity: who should provide and manage the vegetation that is required to protect a sensitive site? Should it be those who create the particle source or those who are adjacent to or upwind of the sensitive site? Expressed another way, should the landholder responsible for a particle source (such as spray drift) also be responsible for extracting as many particles as possible from the air before it leaves the property boundary, or should riparian lands be conserved to offer a “final filter” or “shelter belt” to protect the river? While this report does not attempt to answer these questions, the results have applicability for issues such as these which confront vegetation management committees and the DLWC.

-----

***Acknowledgments:*** This report is one outcome of the Centre for Natural Resources project *Aerial Pathway Study of Nutrient Movement* (PAT2) WPD P3356, within the NSW Department of Land and Water Conservation (DLWC). The work was initiated by a collaborative effort between the Centre for Natural Resources and the first author (MRR) who undertook a preliminary investigative study into the efficiency of vegetation in extracting particles from the air. We thank our colleagues Helen Cleugh, Tom Denmead and Murray Judd for comments on a draft of the report, and Greg Heath and Peter Briggs for assistance with the figures.

## APPENDICES

### Appendix A: Model for Deposition Velocity of Particles to Vegetation

This Appendix supplements Section 2.3 of the main text.

The deposition of particles to a vegetated surface occurs by three processes acting in parallel: direct gravitational settling, inertial impaction and Brownian diffusion. The first models to describe this complex set of processes were "single-layer" models in which the vegetated surface was treated as a bulk entity (Owen and Thomson, 1963; Chamberlain, 1967; Sehmel, 1980). Later work endeavoured to resolve some of the complexities associated with the structure of the vegetation canopy through "multi-layer" models which resolve the vertical variation of the wind field, particle concentration and deposition processes inside the canopy (Bache, 1979a,b; Slinn, 1982; Davidson *et al.*, 1982; Ferrandino and Aylor, 1985; Raupach, 1993). While many of these multi-layer models provide good representations of data from specific experiments, they are too demanding on data and parameterisations to be useful in the present context. Therefore, we use a single-layer model here.

The model is based on antecedents for single-layer models of gas transfer to vegetation (Chamberlain, 1966; 1967; Shreffler, 1978; Hicks *et al.*, 1985), but makes use of more recent understanding of leaf-scale processes as reviewed by Davidson and Wu (1990). The deposition velocity is treated as a bulk (single-layer) conductance made up of three component bulk conductances acting in parallel:

$$W_d = W_t + G_{imp} + G_{brow} \quad (A1)$$

where  $W_t$  (the terminal velocity) accounts for gravitational settling,  $G_{imp}$  for impaction, and  $G_{brow}$  for Brownian diffusion. Of these three,  $W_t$  is a well-known function (eg. Malcolm and Raupach, 1991), and  $G_{imp}$  and  $G_{brow}$  are calculated using the analogy between particle transfer to the surface and momentum transfer.

The bulk aerodynamic conductance for momentum ( $G_{aM} = u_*^2/u_r$ , where  $u_*$  is the friction velocity and  $u_r$  the mean wind speed at the reference level  $z_r$ ) is a known property of the surface which can be specified in terms of the aerodynamic roughness length and thence the architecture of the canopy (Raupach, 1992; 1994). Two processes contribute to  $G_{aM}$ : form or pressure drag, and viscous or skin-friction drag (Thom 1971), so we may write  $G_{aM} = G_{aM}(\text{form}) + G_{aM}(\text{visc})$ . For a typical crop canopy, Thom (1971) estimated the ratio of

the contributions of form and viscous drag to the total drag to be about 3:1. If  $f_{form}$  is the fraction of the total canopy drag exerted as form drag, this implies that  $G_{aM}(\text{form}) = f_{form}G_{aM}$  and  $G_{aM}(\text{visc}) = (1-f_{form})G_{aM}$ , with  $f_{form} = 0.75$ .

We now relate the Brownian conductance  $G_{brow}$  to  $G_{aM}(\text{visc})$ , and the impaction conductance  $G_{imp}$  to  $G_{aM}(\text{form})$ . For  $G_{brow}$ , the hypothesis is

$$G_{brow} = a_v \text{Sc}^{-2/3} G_{aM}(\text{visc}) \quad (\text{A2})$$

where  $\text{Sc}$  is the particle Schmidt number ( $\text{Sc} = \mathbf{n}_a / \mathbf{k}_p$ , where  $\mathbf{n}_a$  is the kinematic viscosity of air and  $\mathbf{k}_p$  the Brownian diffusivity for particles in air), and  $a_v$  is a factor of order 1 accounting for different effects of inter-element sheltering on the molecular transfer of particles and momentum. The factor  $\text{Sc}^{-2/3}$  accounts for the different molecular diffusivities of particles and momentum (Monteith, 1973). The Brownian diffusivity is given as a function of particle diameter  $d$  by the Stokes-Einstein formula (Fuchs, 1964):  $\mathbf{k}_p = (1 + 2.5\lambda_{path}/d)[kT/(3\pi\rho_a\nu_a d)]$ , where  $k$  is the Boltzmann constant,  $T$  the absolute temperature,  $\rho_a$  the air density and  $\lambda_{path}$  the mean free path of air molecules (about  $2 \times 10^{-7}$  m at sea level).

For the particle impaction conductance  $G_{imp}$ , the hypothesis is

$$G_{imp} = a_f E_{imp} G_{aM}(\text{form}) \quad (\text{A3})$$

where  $E_{imp}$  is the particle impaction efficiency ( $0 < E_{imp} < 1$ ) and  $a_f$  is another factor of order 1 accounting for differential sheltering effects. The motivations for Equation (A3) are that a direct analogy between the conductances for particle impaction and form drag is only likely to be valid for particles with impaction efficiencies close to 1, and that the role of particle diameter in impaction can be quantified directly by the impaction efficiency. This can be specified as a function of the Stokes number  $\text{St}$ :

$$E_{imp} = \left( \frac{\text{St}}{\text{St} + p} \right)^q; \quad \text{St} = \frac{2\mathbf{t}_{stoke}U_c}{d_c}; \quad \mathbf{t}_{stoke} = \frac{\mathbf{r}_p d^2}{18\mathbf{r}_a \mathbf{n}_a} \quad (\text{A4})$$

where  $\rho_p$  is the particle density,  $d_c$  is the dimension of the canopy elements upon which impaction occurs, and  $U_c$  is the flow velocity about the canopy elements (characterised by the friction velocity  $u_*$ ). The Stokes number  $\text{St}$  is the ratio of the Stokes relaxation time  $\tau_{stoke}$  to the radial traversal time  $d_c/(2U_c)$ . Equation (A4) uses a commonly assumed empirical form for

the function  $E_{imp}(St)$ , for which Bache (1981) and Peters and Eiden (1992) proposed  $p = 0.8$  and  $q = 2$  for several element shapes on the basis of empirical fits to data.

Combining Equations (A1) to (A4), the final form of the single-layer model for  $W_d$  is

$$W_d = W_t + g_{aM} \left[ f_{form} a_f E_{imp} + (1 - f_{form}) a_v Sc^{-2/3} \right] \quad (A5)$$

in which  $a_f$  and  $a_v$  are parameters to be determined empirically. Tests against the wind tunnel data of Chamberlain (1967), shown in Figure 3, produce optimal agreement when  $a_f = 2$  and  $a_v = 8$  (taking  $f_{form} = 0.75$ ). In the present applications, the particles are sufficiently large that Brownian diffusion is negligible (see Figure 4) so the parameter  $a_v$  has no practical influence and Equation (A5) is effectively a single-parameter model through the product  $f_{form} a_f$ .

Although this model is a great simplification of the real, multi-layer physics, it has advantages for the present purpose: it includes enough physics to capture the dependence of the three major processes (settling, impaction and Brownian diffusion) on particle diameter and wind speed; its two empirical coefficients are sufficient to permit matching to experimental reality but not enough to introduce parameterisation problems; and it makes full use of information about bulk momentum transfer to characterise the aerodynamic properties of the canopy. The behaviour of the model, and tests against wind tunnel data, are described in the main text (Section 2.3).

## Appendix B: Dispersion and Deposition of Particles Over a Nonuniform Surface

This Appendix supplements Section 3 of the main text, describing a model for the dispersion and deposition of a cloud of particles over a patchy or heterogenous surface characterised by a deposition velocity  $W_d$  which is not horizontally uniform. The model is a simple, approximate description based on mass conservation and a Gaussian-plume assumption. The starting point is the conservation equation for particles in the air,

$$\frac{\partial c}{\partial t} + u \frac{\partial c}{\partial x} = -\frac{\partial f_y}{\partial y} - \frac{\partial f_z}{\partial z} + p \quad (\text{B1})$$

where  $x$ ,  $y$ , and  $z$  are along-wind, cross-wind and vertical position coordinates (with  $z = 0$  at the ground),  $t$  is time,  $c$  is the particle concentration,  $\phi_y$  and  $\phi_z$  are the cross-wind and vertical flux densities,  $p$  is the particle source density or release rate (in  $\text{kg m}^{-3} \text{s}^{-1}$ ), and  $u(z)$  is the wind velocity. The quantities  $c$ ,  $p$ ,  $\phi_y$  and  $\phi_z$  are all functions of  $x$ ,  $y$ ,  $z$  and  $t$  in general, but the wind speed  $u$  is assumed to vary only with height  $z$ . In other words, the wind field is steady in time and horizontally homogeneous. This is a significant simplification of the real situation over patchy vegetation, where the wind field varies horizontally.

We restrict attention to ‘‘puff’’ releases of material, defined as releases which are localised in time (but not necessarily instantaneous) so that  $c$ ,  $p$ ,  $\phi_y$  and  $\phi_z$  have finite integrals, as in Equation (1). Then time integration of Equation (B1) yields

$$u \frac{\partial C}{\partial x} = -\frac{\partial \Phi_y}{\partial y} - \frac{\partial \Phi_z}{\partial z} + P \quad (\text{B2})$$

where  $C$ ,  $P$ ,  $\Phi_y$  and  $\Phi_z$  are the time integrals of  $c$ ,  $p$ ,  $\phi_y$  and  $\phi_z$ , as in Equation (1). The time-integrated downward flux at the ground is the deposition  $D(x, y) = -\Phi_z(x, y)$ , with units  $\text{kg m}^{-2}$ . This is specified by a spatially variable deposition velocity  $W_d(x, y)$  such that

$$D(x, y) = W_d(x, y)C_r(x, y) \quad (\text{B3})$$

where  $C_r(x, y) = C(x, y, z_r)$  is the time-integrated (dose) concentration at a low reference height  $z_r$ . Equation (B3) is the lower boundary condition on Equations (B1) and (B2). The initial condition is that  $C$  is zero far upstream and as  $t \rightarrow -\infty$ . We note the congruence between the dose field for a puff release and the concentration field for a steady plume release with the

same source geometry: the former is described by Equation (B2) and the latter by Equation (B1) without the time derivative term, with similar boundary conditions in each case.

Let a mass  $M$  of particles be released from a near-instantaneous source in the  $yz$  plane at  $x = x_s$  (so that  $M$  is the integral of the source density  $p(x,y,z,t)$  over  $x, y, z$  and  $t$ , or the integral of  $P(x,y,z)$  over  $x, y$  and  $z$ ). Recalling that  $C$  is a time-integrated concentration with dimension  $[\text{kg m}^{-3} \text{ s}]$ , the integral mass balance over the  $yz$  plane just downstream of  $x = x_s$  is

$$M = \int_0^{\infty} \int_{-\infty}^{\infty} u(z) C(x_s, y, z) dy dz \quad (\text{B4})$$

Physically, this means that  $M$  equals the total mass of particles (the time-integrated mass flux) crossing the  $yz$  plane just downwind of  $x = x_s$ . However, as the particles travel downwind they are removed by deposition to the surface. To describe this, we consider the mass fraction  $s(x/x_s)$  defined by

$$s(x|x_s) = \frac{1}{M(x_s)} \int_0^{\infty} \int_{-\infty}^{\infty} u(z) C(x, y, z) dy dz \quad (\text{B5})$$

which is the total mass of particles crossing the  $yz$  plane at  $x$ , normalised by the original mass  $M$  released at  $x = x_s$ . Clearly,  $s = 1$  at  $x = x_s$ . An equation for the evolution of  $s(x/x_s)$  can be found by integrating Equation (B2) over the  $yz$  plane. Using Equations (B2) to (B5) and noting that fluxes vanish as  $y \rightarrow \pm\infty$  and  $z \rightarrow +\infty$ , we obtain

$$M \frac{ds(x|x_s)}{dx} = - \int_{-\infty}^{\infty} D(x, y) dy = - \int_{-\infty}^{\infty} W_d(x, y) C(x, y, z_r) dy \quad (\text{B6})$$

which specifies the streamwise evolution of  $s(x/x_s)$ .

It is necessary to close this equation by relating the final concentration integral to  $s(x/x_s)$ . For this purpose, we use two key simplifying assumptions:

1. At each  $x$ , the concentration field in the dispersing and depositing puff is the same as that in a non-depositing but otherwise similar puff containing mass  $M s(x/x_s)$ .
2. The shape of the concentration field is Gaussian in space.

These are the assumptions of the "source-depletion" method (Hanna *et al.*, 1982). They are analysed in the main text, Section 3.3.

In a Gaussian puff from a point release of mass  $M$  at location  $x = x_s$ ,  $y = y_s$  and release height  $z = h_s$ , in a mean wind of speed  $u_r$  along the  $x$  axis, the field of dose concentration (or time integrated concentration) is (Csanady, 1973; Hanna *et al.*, 1982):

$$C(x, y, z | x_s, y_s, h_s) = \frac{M}{2p u_r s_Y s_Z} \exp\left(\frac{-(y - y_s)^2}{2s_Y^2}\right) \left\{ \exp\left(\frac{-(z - z_s)^2}{2s_Z^2}\right) + \exp\left(\frac{-(z + z_s)^2}{2s_Z^2}\right) \right\} \quad (\text{B7})$$

where  $s_Y(x - x_s)$  is the plume width,  $s_Z(x - x_s)$  is the plume depth, and  $z_s(x - x_s)$  is the height of the plume centroid, all defined by the distance  $(x - x_s)$  travelled by the particles to the point  $x$  from the release point  $x_s$ . We can refer to  $s_Y$ ,  $s_Z$  and  $z_s$  as “plume” characteristics because, as noted above, the time-integrated concentration field from a puff is congruent with the concentration in a steady plume. If the particles are settling under gravitation with terminal velocity  $W_t$ , then the plume centroid can be assumed to obey  $z_s(x - x_s) = \max[h_s - (x - x_s)W_t/u, 0]$ , while for a non-settling material such as a gas,  $W_t = 0$  and  $z_s = h_s$ . Empirical forms for  $s_Y$  and  $s_Z$  are often specified in terms of Pasquill stability classes, for example by Hanna *et al.* (1982) as summarised in Table B1.

Pasquill stability class	Plume width $s_Y(x)$ (km)	Plume depth $s_Z(x)$ (km)
Z (super-unstable)	$0.40x(1+0.1x)^{-1/2}$	$0.40x$
A (very unstable)	$0.22x(1+0.1x)^{-1/2}$	$0.20x$
B (moderately unstable)	$0.16x(1+0.1x)^{-1/2}$	$0.12x$
C (slightly unstable)	$0.11x(1+0.1x)^{-1/2}$	$0.08x(1+0.2x)^{-1/2}$
D (neutral)	$0.08x(1+0.1x)^{-1/2}$	$0.06x(1+1.5x)^{-1/2}$
E (slightly stable)	$0.06x(1+0.1x)^{-1/2}$	$0.03x(1+0.3x)^{-1}$
F (moderately stable)	$0.04x(1+0.1x)^{-1/2}$	$0.016x(1+0.3x)^{-1}$

Table B1: Formulae recommended by Hanna *et al.* (1982) for the width  $s_Y(x)$  and depth  $s_Z(x)$  of a Gaussian plume from a point source near the ground, as a function of downwind distance  $x$  (km), valid for  $0.1 < x < 10$  km. A “super-unstable” class Z has been added.

At this point, for simplicity, we assume lateral (cross-wind) homogeneity. This means that both the source distribution and the downwind surface are uniform in the lateral ( $y$ ) dimension, consisting of long cross-wind strips, so that the source distribution and the deposition pattern are functions of  $x$  only. Then, substitution of Equation (B7) into (B6) and integration in  $y$  yields an ordinary differential equation for  $s(x|x_s)$ :

$$\frac{ds(x|x_s)}{dx} = -\left(\frac{2}{p}\right)^{1/2} \frac{W_d(x)s(x|x_s)}{u_r \mathbf{s}_Z(x-x_s)} \exp\left[\frac{-z_s^2(x-x_s)}{2\mathbf{s}_Z^2(x-x_s)}\right] \quad (\text{B8})$$

The initial condition is  $s = 1$  at  $x = x_s$ . Equation (B8) is easily solved numerically (for instance using the Runge-Kutta method) once  $h_s$ ,  $u$ ,  $W_t$ ,  $W_d(x)$  and  $\mathbf{s}_Z(x-x_s)$  are specified. Of these,  $h_s$  and  $u$  are measured parameters, and  $\mathbf{s}_Z(x-x_s)$  is given in Table B1. The terminal velocity  $W_t$  is zero for a gas, while for particles it depends on particle diameter, particle-to-air density ratio and air viscosity, and can be calculated by standard methods summarised in Malcolm and Raupach (1991). The deposition velocity  $W_d(x)$  depends on particle diameter, wind speed and the properties of the vegetation at the point  $x$ , according to the model given in Appendix A.

Having determined  $s(x|x_s)$  by solving Equation (B8), the next step is to find the deposition  $D_1(x|x_s)$  for a unit lateral line source (a particle release of 1 kg per y-metre along a line across the wind) at the point  $x_s$ . This is given from Equation (B6), with  $M = 1$  kg and after integration in  $y$ , by

$$D_1(x|x_s) = -\frac{ds(x|x_s)}{dx} \quad (\text{B9})$$

An equivalent form follows from Equations (B3) and (B7), after integration in  $y$  and with  $M$  replaced by  $s(x|x_s)$  under the source-depletion approximation for a unit lateral line source. These operations yield

$$\begin{aligned} D_1(x|x_s) &= W_d(x) C_1(x|x_s); \\ C_1(x|x_s) &= \left(\frac{2}{p}\right)^{1/2} \frac{s(x|x_s)}{u_r \mathbf{s}_Z(x-x_s)} \exp\left(\frac{-z_s^2(x-x_s)}{2\mathbf{s}_Z^2(x-x_s)}\right) \end{aligned} \quad (\text{B10})$$

where  $C_1(x|x_s)$  is the dose concentration from the unit lateral line source at  $x_s$ .

Finally, the deposition for a plane source of dose  $Q$  ( $\text{kg m}^{-2}$ ) can be obtained by integrating the line-source deposition  $D(x)$  for an array of lateral line sources which together make up a plane source, just as individual spray swathes together cover a cotton field. This deposition can be characterised by the deposition fraction  $D(x)/Q$ , the actual deposition normalised by the dose released at the plane source (denoted  $f_{drift}$  in Raupach *et al.* 1999a,b)). If the plane source extends uniformly from  $x = -x_p$  to  $x = 0$ , then the deposition fraction is

$$\frac{D(x)}{Q} = \int_{-x_p}^0 D_1(x|x_s) dx_s \quad (\text{B11})$$

where  $D_1(x|x_s)$  is given by either Equation (B9) or (B10).

In the special case where the underlying surface is uniform,  $W_d$  is independent of  $x$  and  $s(x/x_s) = s(x - x_s)$ , so that Equation (B11) reduces to

$$\frac{D(x)}{Q} = - \int_{-x_p}^0 \frac{ds(x - x_s)}{dx} dx_s = s(x) - s(x + x_p) \quad (\text{B12})$$

as in Raupach *et al.* (1999b). However, this expression is not applicable more generally when the underlying surface is not uniform and  $W_d$  depends on  $x$ .

In practice we are usually concerned with the dispersion of a cloud containing a distribution  $P(d)$  of particle sizes where  $d$  is the particle diameter. Particle size influences  $s(x)$  and thence the deposition  $D$  through the deposition velocity  $W_d$ , which is a strong function of  $d$  (Appendix A). Hence the deposition is calculated separately for each particle size and summing the results, weighted by  $P(d)$ .

The behaviour of this model, and tests against field data for the case of a uniform underlying surface, are described in the main text (Section 3.2).

## Appendix C: Approximate Determination of Leaf Area Index

This Appendix gives approximate formulae for determining Leaf Area Index (LAI) from visual and geometrical properties of a canopy.

**Closed Canopies:** The key properties are the canopy height ( $h_c$ ) and the "transmission distance" ( $X_e$ ), the mean distance through the canopy over which the optical transmission is  $1/e = 0.368$ , or roughly  $1/3$ . Rough visual estimates of both of these quantities can be made. In the case of  $X_e$ , one estimates the distance through the canopy at which  $2/3$  of an object (such as a white card) is obscured by intervening leaves and stems, and  $1/3$  is visible. It is necessary to account for trunk spaces and non-uniformity of the vegetation with height, which can be done roughly by estimating  $X_e$  visually along sloping rays through the canopy.

The Frontal Area Index (FAI) is defined as the frontal area of vegetation elements (as seen from the wind direction) per unit ground area. This is given by

$$\text{FAI} = h_c / X_e \quad (\text{C1})$$

Then, LAI can be estimated as twice the FAI. The ratio  $\text{LAI}/\text{FAI} = 2$  is exact for a canopy in which the all elements are flat plates isotropically oriented (equally likely to be facing in any direction). For other canopies, it is reasonable to take  $\text{LAI}/\text{FAI} = 2$  as a first approximation.

**Open canopies:** Let there be  $N$  trees per unit area, and let the horizontal dimension of each tree be  $D$ . Then the projected area occupied by each tree is  $D^2$  and the volume of each tree is  $h_c D^2$ . (We neglect factors of  $\pi/4$  or  $\pi/6$  which would respectively account for cylindrical or spherical shapes). If the transmission distance *through a tree crown* is  $X_e$ , then

$$\text{FAI} = \frac{h_c D^2 N}{X_e}; \quad \text{LAI} \approx 2 \times \text{FAI} \quad (\text{C2})$$

As examples, typical values of  $X_e$  might be 1, 3 or 10 m for a dense, medium or open tree crown, respectively. Suppose that there are 10 trees per hectare ( $N = 0.001 \text{ m}^{-2}$ ) with  $h_c = 2$  m,  $D = 2$  m and  $X_e = 3$  m (medium). Then  $\text{LAI} \approx 0.005$ . If there are 100 stems per hectare with  $h_c = 2$  m,  $D = 2$  m and  $X_e = 1$  m (dense), then  $\text{LAI} \approx 0.08$ .

An even rougher approximation can be obtained by assuming that  $h_c$  and  $X_e$  are about the same (a reasonable starting point). Then  $\text{LAI} \approx 2D^2/N$ . The fraction  $D^2/N$  is the cover fraction of the canopy, so according to this estimate, LAI is twice the cover fraction.

## REFERENCES

- Arya, S.P.S. (1975). A drag partition theory for determining the large-scale roughness parameter and wind stress on the Arctic pack ice. *J. Geophys. Res.* **80**, 3447-3454.
- Bache, D.H. 1979a. Particle transport within plant canopies - I. A framework for analysis. *Atmos. Environ.* **13**, 1257-1262.
- Bache, D.H. 1979b. Particulate transport within plant canopies - II. Prediction of deposition velocities. *Atmos. Environ.* **13**, 1681-1687.
- Bache, D.H. 1981. Analysing particulate deposition to plant canopies. *Atmos. Environ.* **15**, 1759-1761.
- Bird, S.L., D.M. Esterly, and S.G. Perry. 1996. Off-target deposition of pesticides from agricultural aerial spray applications. *J. Environ. Qual.* **25**, 1095-1104.
- Chamberlain, A.C. 1966. Transport of gases to and from grass and grass-like surfaces. *Proc. Roy. Soc. London* **A290**, 236-265.
- Chamberlain, A.C. 1967. Transport of *Lycopodium* spores and other small particles to rough surfaces. *Proc. Roy. Soc. London* **A296**, 45-70.
- Csanady, G.T. 1973. *Turbulent Diffusion in the Environment*. D. Reidel Publ. Co. Dordrecht.
- Davidson, C.I., J.M. Miller, and M.A. Pleskow. 1982. Influence of surface structure on predicted particle dry deposition to natural grass canopies. *Water Air Soil Poll.* **18**, 25-43.
- Davidson C.I., and Y.L. Wu. 1990. Dry deposition of particles and vapors. p. 103-216. In: S.E. Lindberg, A.L. Page, and S.A. Norton (Eds.) *Acidic Precipitation, Vol. 3: Sources, Deposition, and Canopy Interactions*. Springer-Verlag, New York.
- Ferrandino, F.J. and D.E. Aylor. 1985. An explicit equation for deposition velocity. *Boundary-Layer Meteorol.* **31**, 197-201.
- Fuchs, N.A. 1964. *The Mechanics of Aerosols*. Pergamon Press, Oxford.
- Hanna, S.R., G.A. Briggs, and R.P. Hosker. 1982. *Handbook on Atmospheric Diffusion*. Technical Information Center, U.S. Department of Energy, Oak Ridge.
- Hicks, B.B., D.D. Baldocchi, R.P. Hosker Jr., B.A. Hutchison, D.R. Matt, R.T. McMillen, and L.C. Satterfield. 1985. On the use of monitored air concentrations to infer dry deposition. NOAA Tech. Memorandum ERL ARL-141 Silver Spring, MD.
- Judd, M.J., Raupach, M.R. and Finnigan, J.J. (1996). A wind tunnel study of turbulent flow around single and multiple windbreaks, Part I: velocity fields. *Boundary-Layer Meteorol.* **80**, 127-165.
- Malcolm, L.P. and M.R. Raupach. 1991. Measurements in an air settling tube of the terminal velocity distribution of soil material. *J. Geophys. Res.* **96**, 15275-15286.
- Monteith, J.L. 1973. *Principles of Environmental Physics*. Arnold, London.
- Owen, P.R. and W.R. Thomson. 1963. Heat transfer across rough surfaces. *J. Fluid Mech.* **15**, 321-334.
- Peters, K. and R. Eiden. 1992. Modelling the dry deposition velocity of aerosol particles to a spruce forest. *Atmos. Environ.* **26A**, 2555-2564.

- Raupach, M.R. 1992. Drag and drag partition on rough surfaces. *Boundary-Layer Meteorol.* **60**, 375-395. [Corrigendum: *Boundary-Layer Meteorol.* **76**, 303-304 (1995)]
- Raupach, M.R. 1993. Dry deposition of gases and particles to vegetation. *Clean Air* **27**, 200-203.
- Raupach, M.R. 1994. Simplified expressions for vegetation roughness length and zero-plane displacement as functions of canopy height and area index. *Boundary-Layer Meteorol.* **71**, 211-216. [Corrigendum: *Boundary-Layer Meteorol.* **76**, 303-304 (1995)]
- Raupach, M.R., Briggs, P.R., Ford, P.W., Leys, J.F., Muschal, M. and Cooper, B. (1999a). Endosulfan transport I: Integrative assessment of airborne and waterborne pathways. *Journal of Environmental Quality* (Submitted).
- Raupach, M.R., Briggs, P.R., Ahmad, N. and Edge, V. (1999b). Endosulfan transport II: Modelling airborne dispersal and deposition by spray and vapour. *Journal of Environmental Quality* (Submitted).
- Schofield *et al.* (1999)
- Sehmel, G.A. 1980. Particle and gas dry deposition: A review. *Atmos. Environ.* **14**, 983-1011.
- Shreffler, J.H. 1978. Factors affecting dry deposition of SO<sub>2</sub> on forests and grasslands. *Atmos. Environ.* **12**, 1497-1503.
- Slinn, W.G.N. 1982. Predictions for particle deposition to vegetative canopies. *Atmos. Environ.* **16**, 1785-1794.
- Thom, A.S. 1971. Momentum absorption by vegetation. *Quart. J. Roy. Meteorol. Soc.* **97**, 414-428.

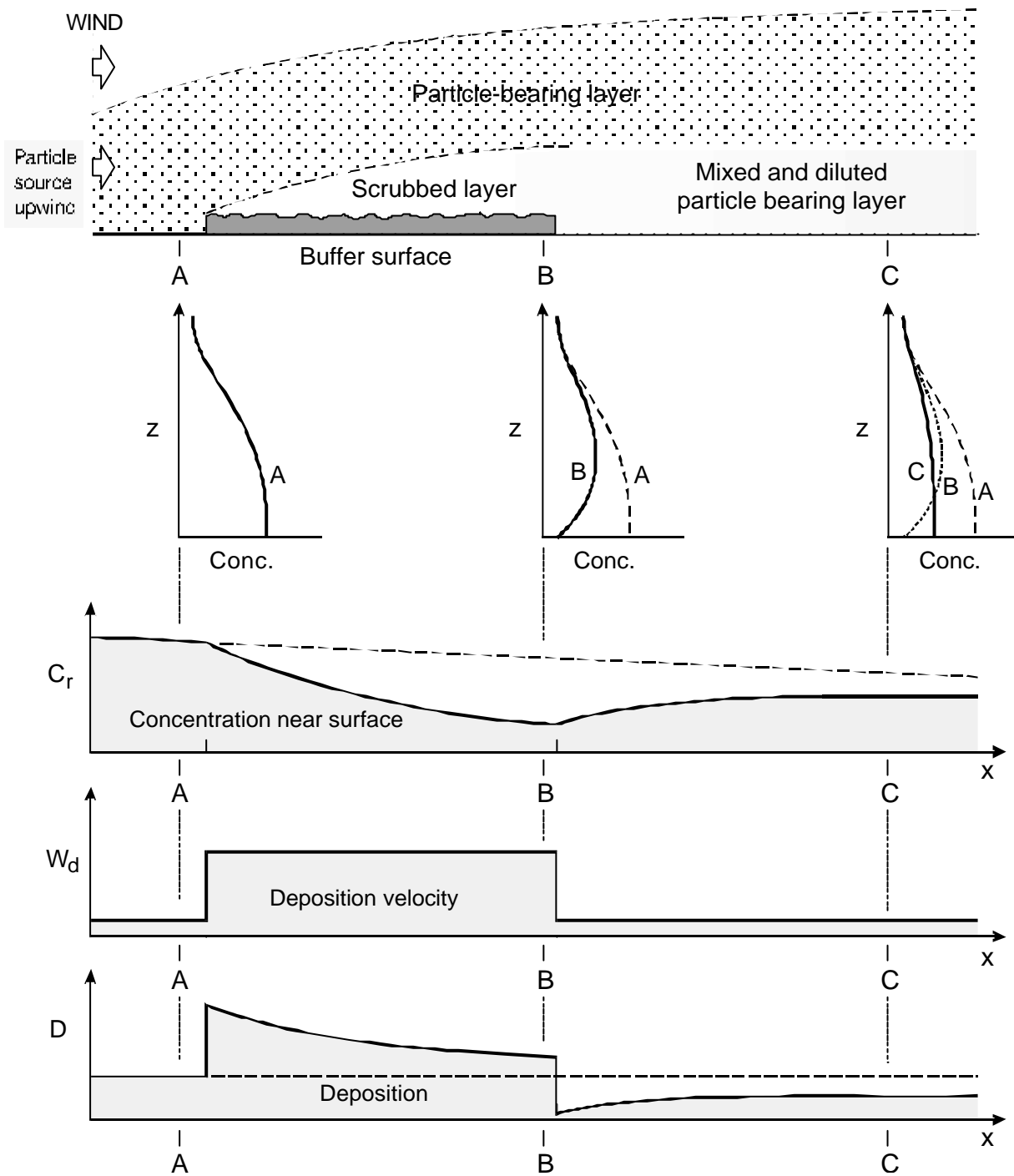


Figure 1: Schematic diagram illustrating mechanism of regional protection against particle deposition to downwind surfaces by a buffer surface with a high potential for particle capture.

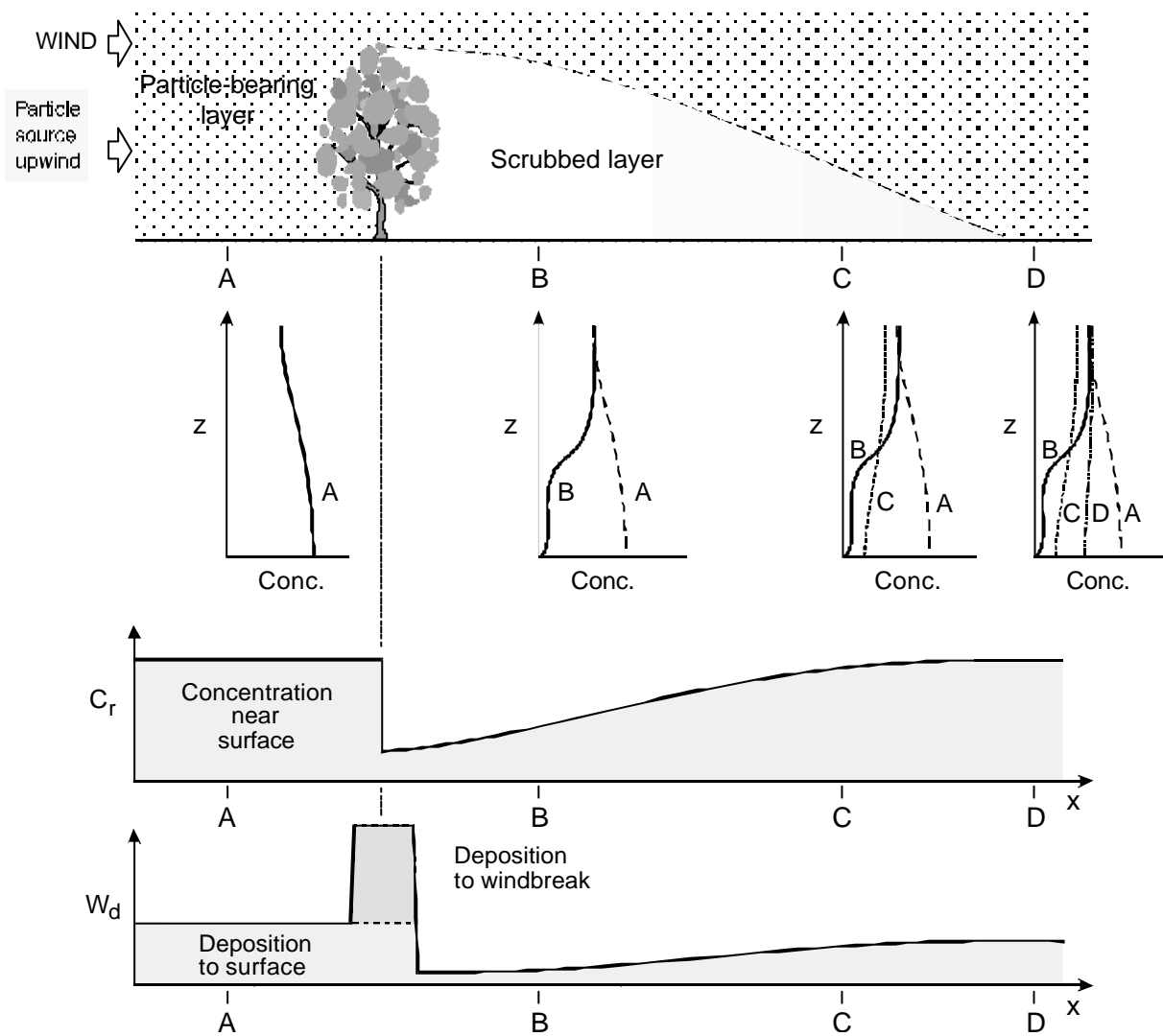


Figure 2: Schematic diagram illustrating mechanism of local protection against particle deposition to downwind surfaces by a porous barrier.

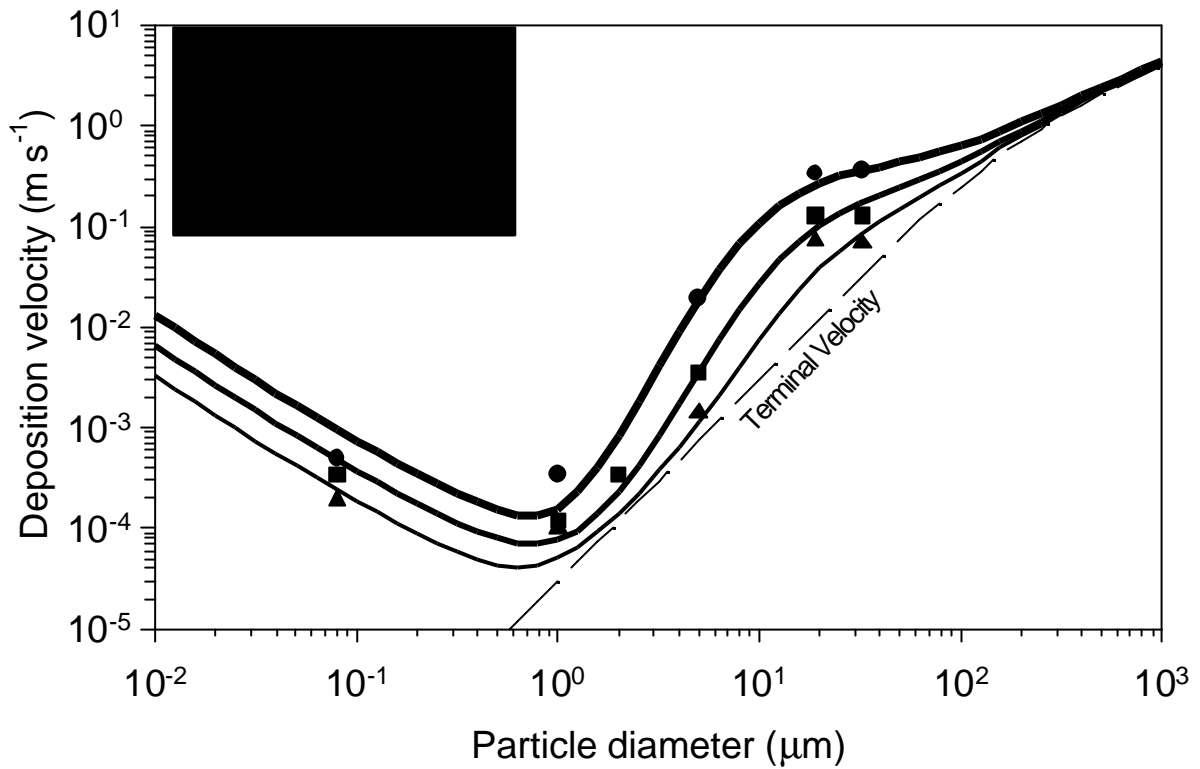


Figure 3: Test of the single-layer model for the deposition velocity  $W_d$ , Equation (A5), against wind tunnel measurements of particle deposition to a sticky grass surface by Chamberlain (1967). Predictions are of  $W_d$  as a function of particle diameter  $d$  for vegetation of height 0.06 m and leaf area index 1, using the model of Raupach (1992, 1994) to calculate roughness length and other canopy aerodynamic properties. Data and predictions are for three wind speeds giving friction velocities ( $u_*$ ) of 0.35, 0.70 and 1.40 m s<sup>-1</sup>. The dashed line is the predicted terminal velocity  $W_t$  as a function of  $d$  (Malcolm and Raupach 1991).

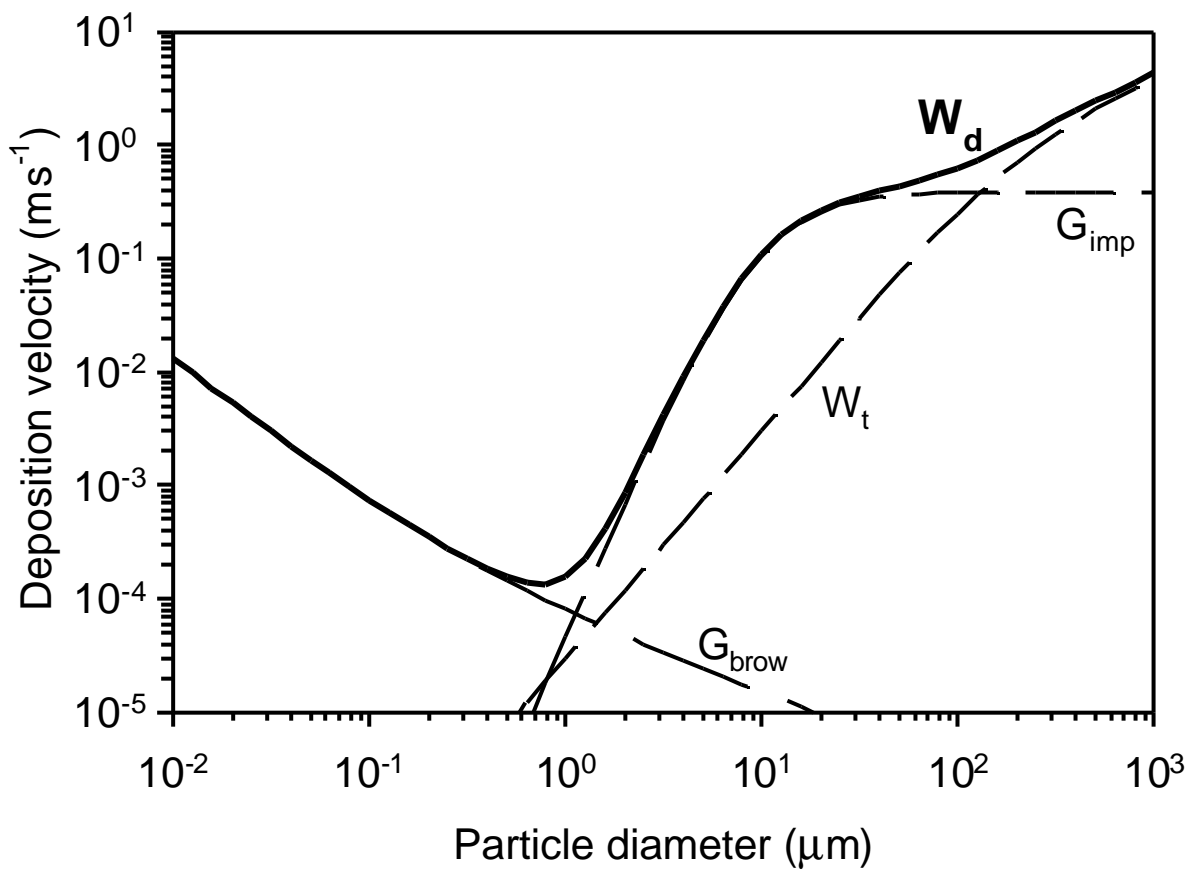


Figure 4: Contributions of the three terms  $W_t$  (settling),  $G_{\text{imp}}$  (impaction) and  $G_{\text{brow}}$  (Brownian diffusion) to the deposition velocity  $W_d$ . Conditions as in Figure 1 with  $u_* = 1.40 \text{ m s}^{-1}$ .

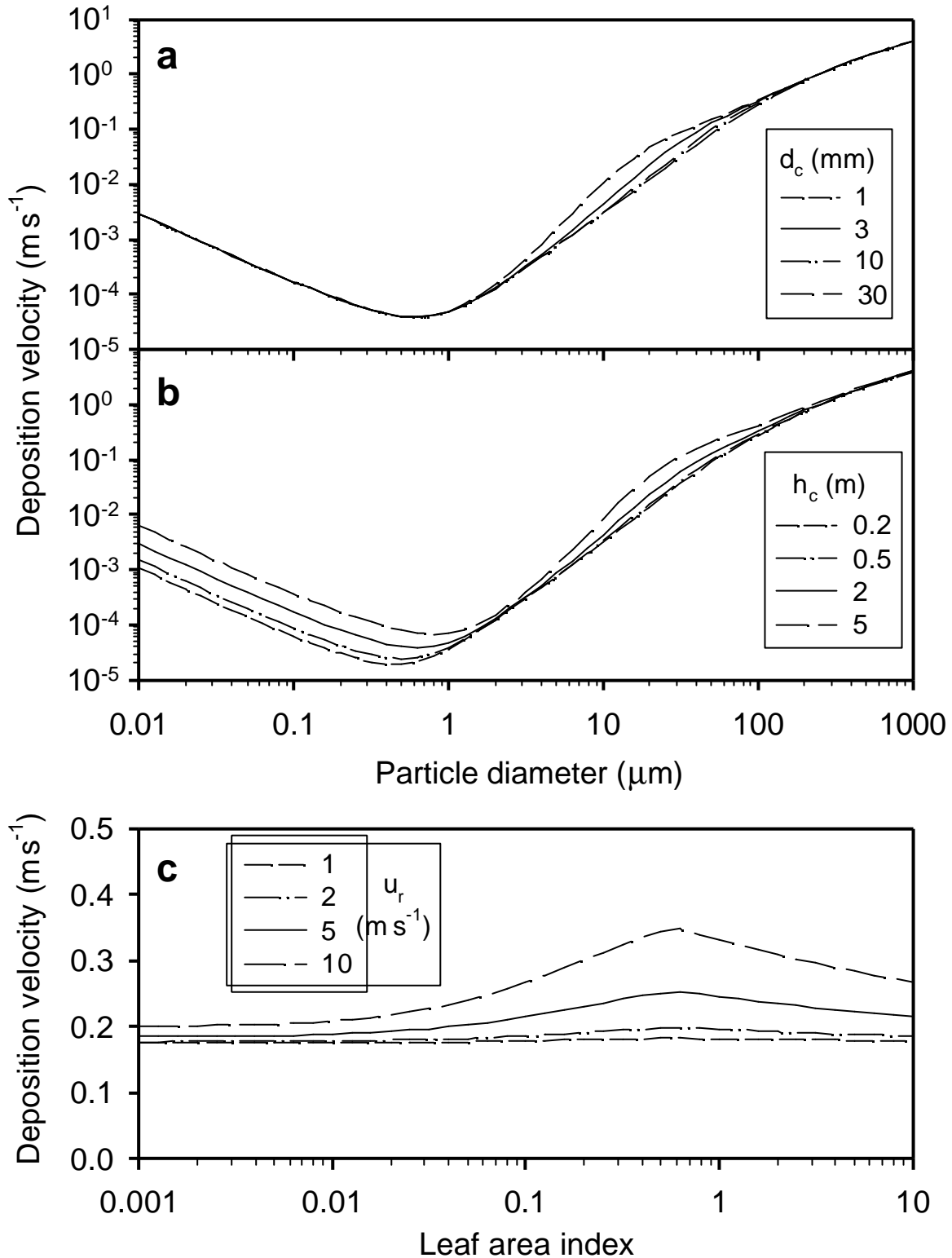


Figure 5: Sensitivity of modelled deposition velocity  $W_d$  (from Equation (A5)) to variation of particle diameter ( $d_p$ ), canopy element dimension ( $d_c$ ), canopy height ( $h_c$ ), leaf area index (LAI) and wind speed ( $u_r$ ) at a reference height  $z_r = 10$  m. Conditions assumed for non-varying parameters:  $d_p = 80$   $\mu\text{m}$ ,  $d_c = 3$  mm,  $h_c = 2$  m,  $u_r = 5$   $\text{m s}^{-1}$ , LAI = 1. (a) Plot of  $W_d$  against  $d_p$  for several values of  $d_c$ ; (b) Plot of  $W_d$  against  $d_p$  for several values of  $h_c$ ; (c) plot of  $W_d$  against LAI for several values of  $u_r$ .

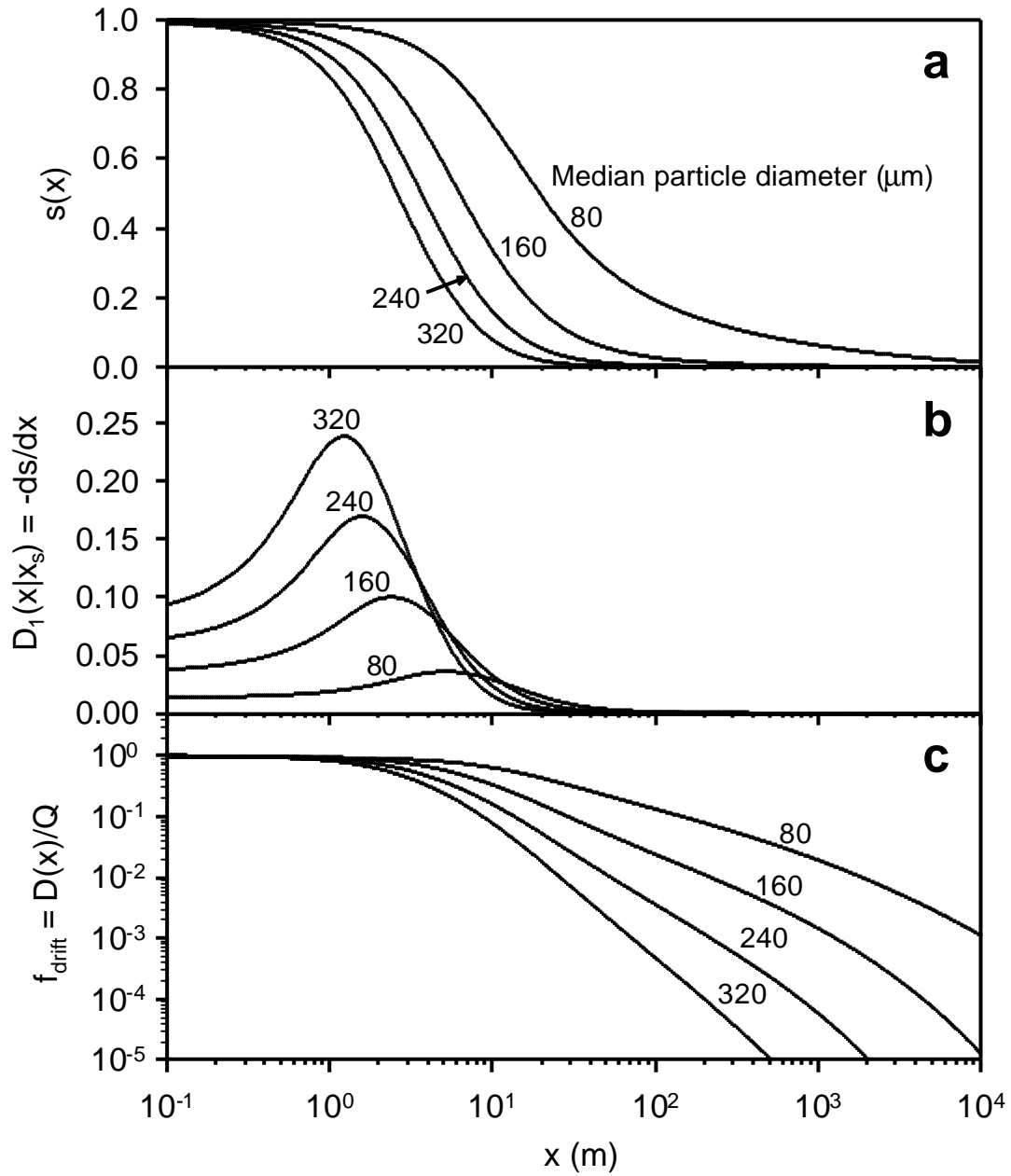


Figure 6: Results from particle dispersion model for four different particle size distributions (log-normal with median particle diameter = 80, 160, 240 and 320  $\mu\text{m}$ ; and standard deviations of  $\ln(d) = \ln(1.8)$  throughout). Conditions assumed throughout: canopy height  $h_c = 0.50$  m; leaf dimension  $d_c = 0.01$  m; field length  $x_p = 1000$  m; spray release height  $h_s = 2$  m; initial plume height  $\sigma_{z0} = 1$  m; atmospheric stability is neutral (class D); wind speed  $u_r = 2$  m  $\text{s}^{-1}$ . Panels: (a) depleting mass fraction  $s(x)$ ; (b) deposition  $D_1(x|x_s)$  for a unit lateral line source at  $x_s = 0$ ; (c) deposition fraction  $D(x)/Q$  for a plane source.

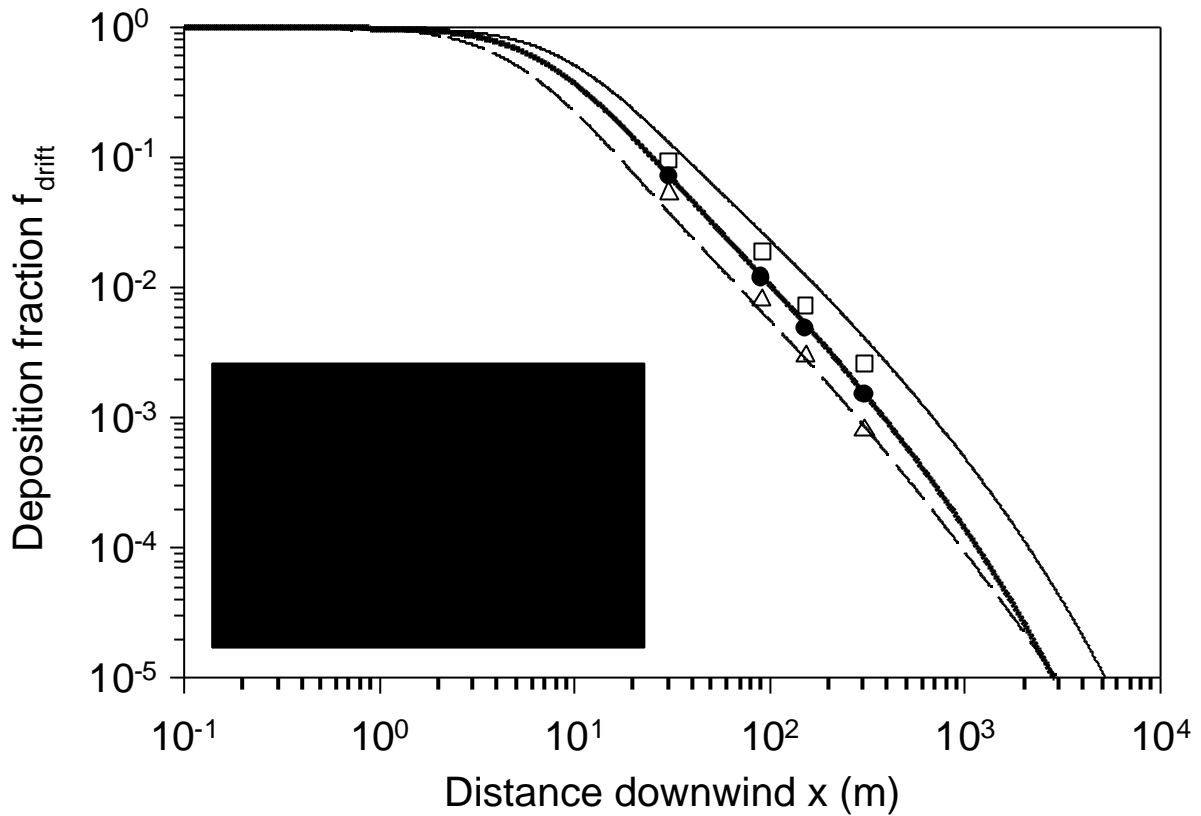


Figure 7: Comparison of particle dispersion (spray drift) model with data from Bird *et al.* (1996, standard case) for three wind speeds  $u$ . Parameters: canopy height  $h_c = 0.15$  m; leaf dimension  $d_c = 0.005$  m; field length  $x_p = 274$  m; spray release height  $h_s = 2.5$  m; initial plume height  $\sigma_{z0} = 1$  m; median particle diameter =  $250 \mu\text{m}$ ; particle size distribution is log-normal with standard deviation of  $\ln(d) = \ln(1.7)$ ; atmospheric stability is neutral (D) or slightly unstable (C).

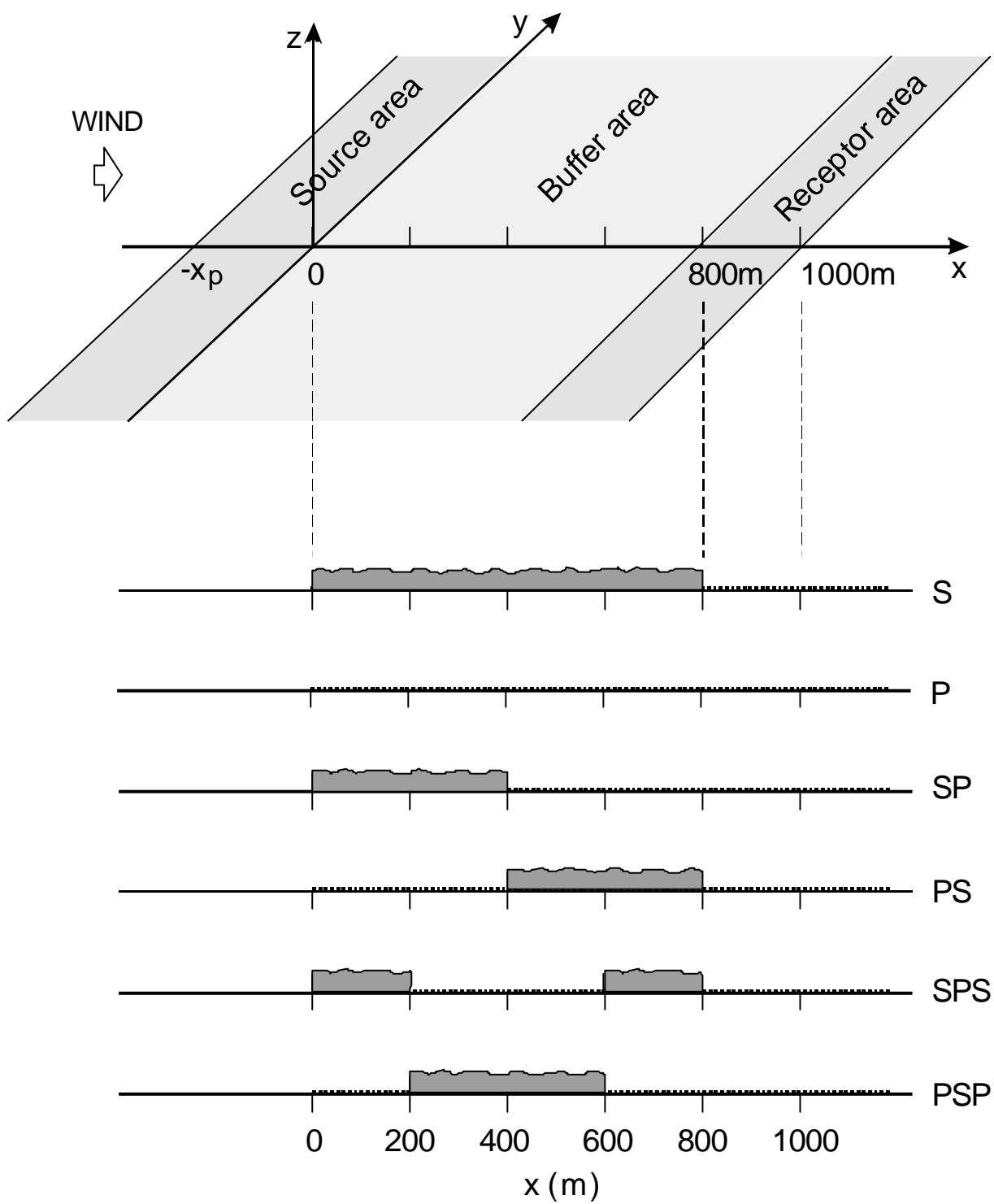


Figure 8: Scenarios used in model assessments of regional protection.

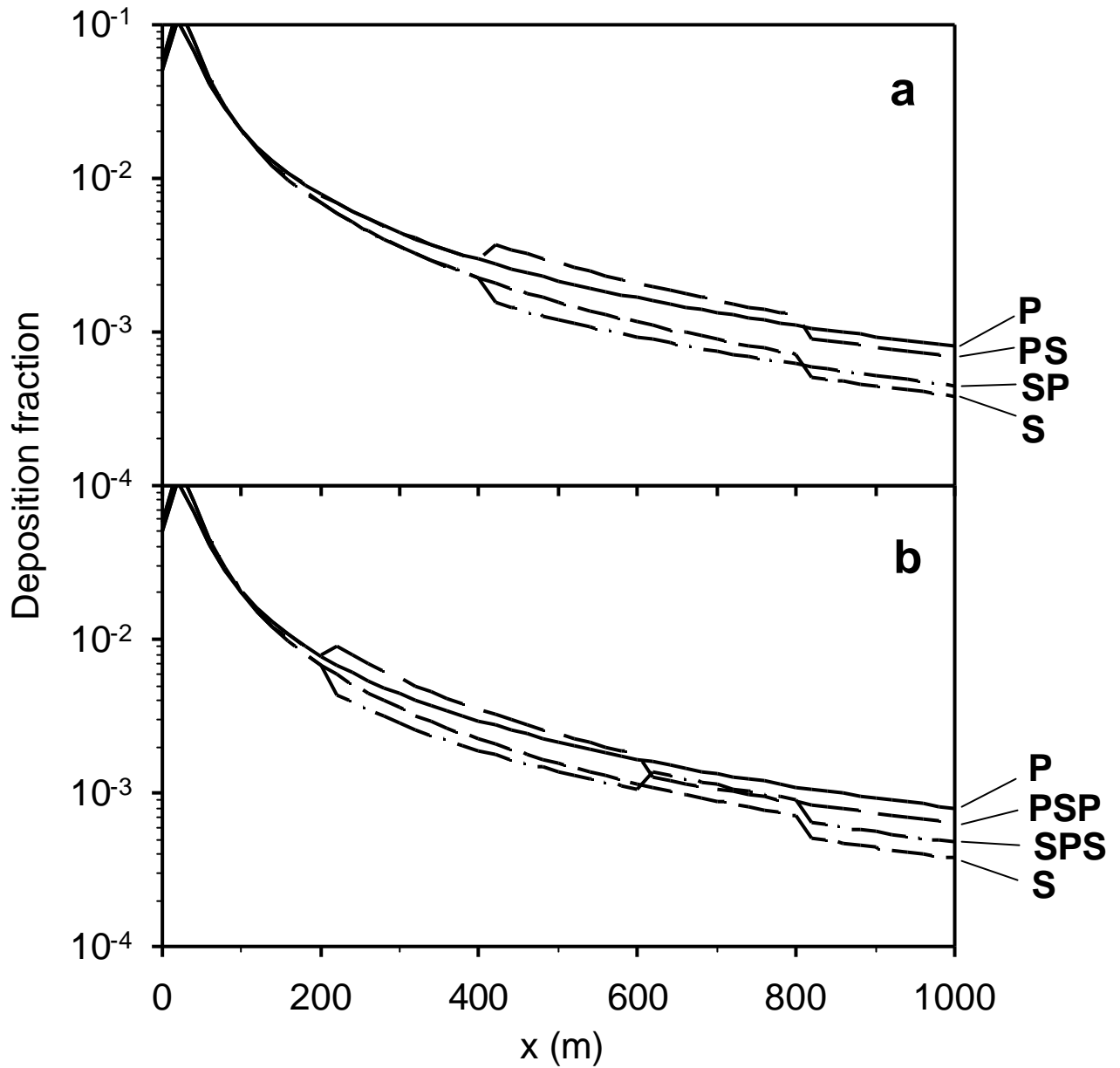


Figure 9: Dependence of deposition fraction  $D(x)/Q$  on distance  $x$  from downwind edge of source area. Source: spray (particle diameter  $d = 80 \mu\text{m}$ ); source dimension  $x_p = 10 \text{ m}$ ; meteorological conditions as specified in text. (a): configurations P, S, SP, PS; (b) configurations P, S, SPS, PSP.

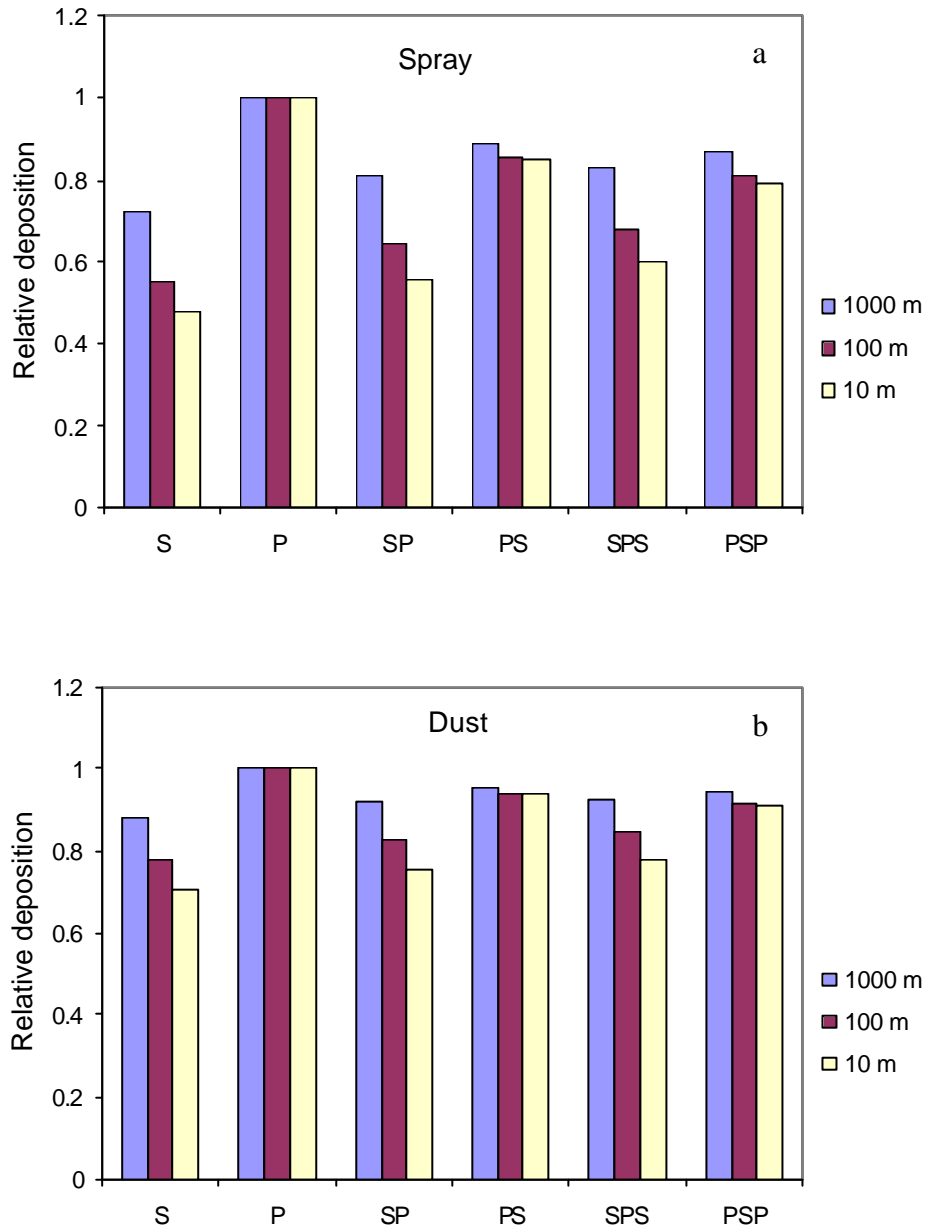


Figure 10: Relative deposition on the receptor (pasture at  $x = 1000$  m) for alternative buffer configurations. Depositions are normalised by the "worst-case" deposition when the buffer area is entirely pasture (P). For each buffer configuration, the three bars represent different source dimensions  $x_p$  (1000 m, 100 m or 10 m). (a) spray; (b) dust.

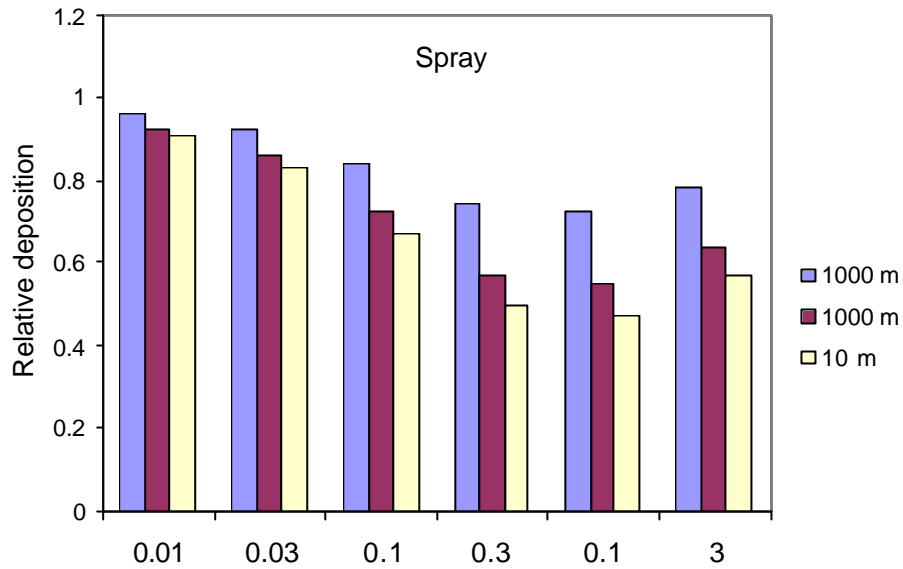


Figure 11: Relative deposition on the receptor (pasture at  $x = 1000$  m) for the shrub buffer (configuration S), for three different atmospheric stabilities: unstable (class A), neutral (class D) and stable class F). Depositions are normalised by the deposition for a pasture buffer (configuration P) under similar stability conditions. For each case, the three bars represent different source dimensions  $x_p$  (1000 m, 100 m or 10 m).

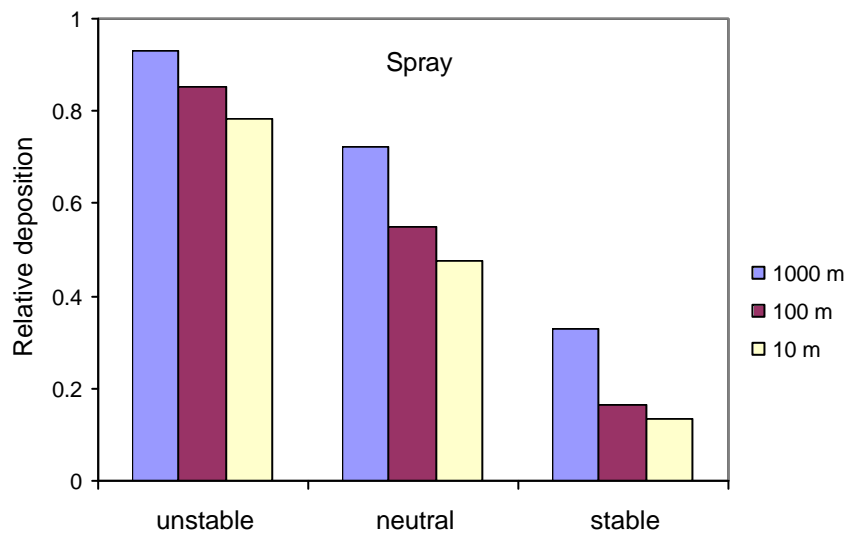


Figure 12: Deposition on the receptor (pasture at  $x = 1000$  m) for the shrub buffer configuration (S) with a range of values of shrub leaf area index (LAI), normalised by the deposition when the buffer area is entirely pasture (P). For each LAI value, the three bars represent different source dimensions  $x_p$  (1000 m, 100 m or 10 m).